Cornichon:
An ancient ER cargo exporter is recruited to serve as an AMPA receptor auxiliary subunit

INAUGURAL-DISSERTATION

zur Erlangung des Doktorgrades
der Mathematisch-Naturwissenschaftlichen Fakultät
der Heinrich-Heine-Universität Düsseldorf

vorgelegt von

Veronika Mauric
aus Pilsen

Düsseldorf, Juni 2013

aus dem Institut für Neuro- und Sinnesphysiologie
der Heinrich-Heine Universität Düsseldorf

Gedruckt mit der Genehmigung der
Mathematisch-Naturwissenschaftlichen Fakultät der
Heinrich-Heine-Universität Düsseldorf

Referent: Prof. Dr. med. Nikolaj Klöcker, Heinrich-Heine-Universität Düsseldorf
Korreferentin: Prof. Dr. rer. nat. Christine R. Rose, Heinrich-Heine-Universität Düsseldorf

Tag der mündlichen Prüfung: 12. Juli 2013

Table of content

Abbreviations

ADAR	Adenosine deaminase that acts on RNA
AMPAR	Alpha-amino-3-hydroxy-5-methyl-4-isoxazole propionic Acid receptor
Axl2p	Axial budding pattern protein
Ca^{2+}	Calcium
CKAMP44	Cystine-knot AMPAR modulating protein of 44 kDa
CNIH-2/3	Cornichon protein-2 and -3
CNS	Central nervous system
COPII	Coat protein complex II
CP	Neocortical Plate
CTD	Carboxyl-terminal domain
DNA	Deoxyribonucleic acid
E	Embryonic day
ECL	Enhanced chemiluminescent
EGF	Epidermal growth factor
EGL	External granule cell layer
ER	Endoplasmic reticulum
Erv14p	ER–vesicle protein of 14 kDa
Fig.	Figure
G / S / M	Cell cycle transitions (gap / synthesis / mitosis)
GABA	Gamma-aminobutyric acid
GalTase	Beta-1,4-Galactosyltransferase
GFP	Green fluorescent protein
GluA	AMPAR subunit
GM130	Golgi matrix protein of 130 kDa
GTP	Guanosine 5'-triphosphate
HB-EGF	Heparin binding epidermal growth factor
HEK	Human embryonic kidney, cell line
HeLa	Henrietta Lacks, cervix carcinoma cell line
IGL	Internal granule cell layer
IZ	Intermediate Zone
KAR	Kainate acid receptor
LBD	Ligand binding domain
mRNA	Messenger ribonucleic Acid

MZ	Molecular Zone
NMDAR	N-methyl-D-aspartate receptor
O2-A	Oligodendrocyte type 2 progenitor
OK	Oppossum kidney, cell line
P	Postnatal day
PCR	Polymerase chain reaction
PDZ	PSD95, Drosophila disc large tumor suppressor (Dlg1), and zonula occludens-1 protein (zo-1)
PL	Purkinje cell layer
PSD93/95	Postsynaptic density protein of 93/95 kDa
PVDF	Polyvinylidene difluoride
Q	Glutamine
R	Arginine
RT-PCR	Reverse transcriptase-polymerase chain reaction
Sar1	Secretion-associated and Ras-related protein 1
SDS-PAGE	Sodium dodecyl sulfate polyacrylamide gel electrophoresis
T	Tween
TARP	Transmembrane AMPA receptor regulatory protein
TBS	Tris-buffered saline
TGF-α	Transforming growth factor alpha
TMD	Transmembrane domain
V	Volt
VZ	Ventricular Zone
WT	wild-type

1. Introduction

1.1 Glutamate receptors

In the mammalian central nervous system (CNS), information processing and distribution relies on excitatory and inhibitory neurotransmission. In the adult brain, glutamate is the most common excitatory neurotransmitter, which is released into the synaptic cleft upon depolarization of the presynaptic nerve terminal. It acts as a ligand at two groups of glutamate receptors: the ionotropic glutamate receptors, which are ligand-gated ion channels and the G-protein-coupled metabotropic receptors, which signal via intracellular second messenger pathways. The metabotropic glutamate receptors forward signals in slow fashion, while the ionotropic relay information much faster.

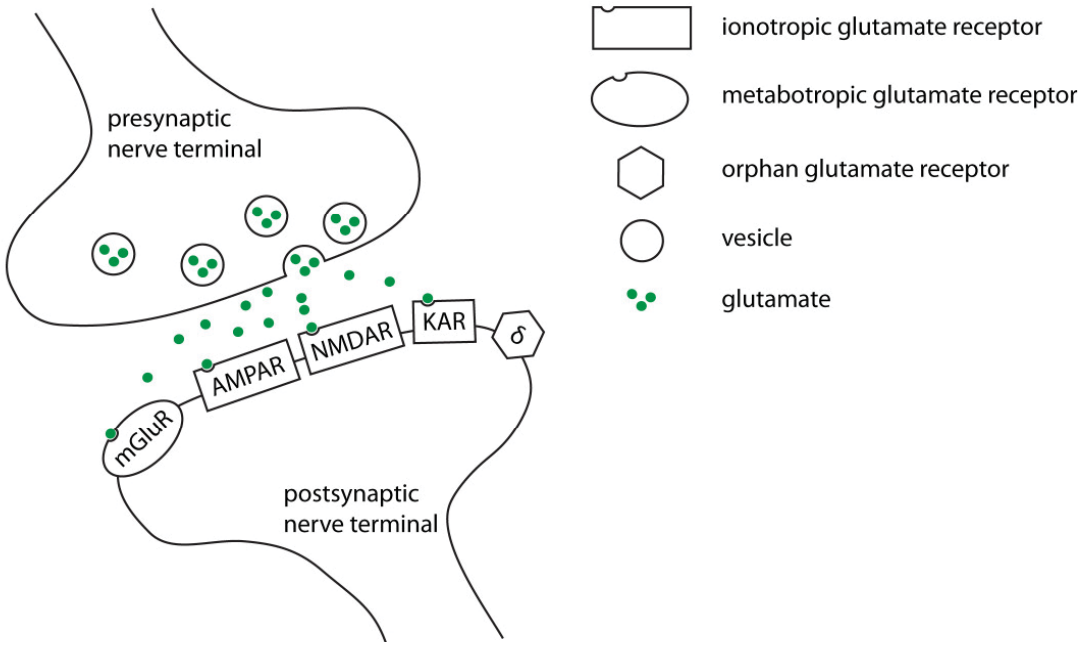

Fig. 1-1. Schematic diagram of a glutamatergic synapse.
Glutamate is released from the presynaptic nerve terminal and activates ionotropic and metabotropic glutamate receptors. Ionotropic receptors are ligand gated ion channels comprised of AMPA, NMDA and kainate receptors. The orphan glutamate receptor is regarded as a glutamate receptor, solely based on sequence homology with the ionotropic glutamate receptors.

Ionotropic glutamate receptors are integral membrane proteins and can be divided into three subtypes, based on their pharmacological and electrophysiological characteristics and comprise the N-methyl-d-aspartate receptor (NMDAR), the α-amino-3-hydroxy-5-

methyl-4-isoxazolepropionic acid receptor (AMPAR) and the kainate receptor (Traynelis, Wollmuth et al. 2010). The orphan δ receptor shares sequence homology with the other ionotropic glutamate receptors, but does neither bind glutamate nor AMPA or NMDA (Lomeli, Sprengel et al. 1993).

All ionotropic glutamate receptors are composed of four subunits (Rosenmund, Stern-Bach et al. 1998), from the same functional receptor class (Leuschner and Hoch 1999), that build the ion channel pore.

Fast excitatory neurotransmission and basal neurotransmission at resting conditions relies on the AMPAR and can be necessary for magnesium unblocking of the NMDAR receptor, that displays slower gating properties. Kainate receptors (KARs) might function rather as supporters than mediators of synaptic transmission (Frerking and Nicoll 2000).

1.2 AMPAR composition, molecular diversity and expression

Native AMPARs exist as tetrameric heteromers, assembled in a dimer of dimers (Tichelaar, Safferling et al. 2004) fashion of the four pore forming α-subunits GluA1 – GluA4 (Hollmann and Heinemann 1994). Only a small subpopulation might also exist in a homomeric fashion (Wenthold, Petralia et al. 1996), (Suzuki, Kessler et al. 2008).

Each GluA subunit comprises a large, extracellular **a**mino-**t**erminal **d**omain (ATD), the extracellular **l**igand **b**inding **d**omain (LBD), three **t**rans**m**embrane **d**omains, (TMD A-C) a pore lining intramembrane helix (pore-loop) and an intracellular **c**arboxy-**t**erminal **d**omain (Traynelis, Wollmuth et al. 2010). The ATD is involved in the first, subfamily-specific assembly step of dimerization (Ayalon and Stern-Bach 2001) and, when exposed to the synaptic cleft, may regulate presynaptic inputs transsynaptically via protein-protein interactions (Ripley, Otto et al. 2011). The three transmembrane segments (Hollmann, Maron et al. 1994) also participate in subunit assembly; additionally, the TMD C has been shown to be implicated in channel gating and desensitization (Terhag, Gottschling et al. 2010). The LBD undergoes a conformational change upon agonist binding, which subsequently leads to channel opening (Stern-Bach, Bettler et al. 1994). Besides, the LBD is implicated in the dimer-to-tetramer transition (Greger, Akamine et al. 2006) and in testing gating transitions in the ER. Exercising gating transitions ensures correct configuration and function, and is therefore crucial for forward trafficking of the AMPAR (Penn, Williams et al. 2008). The CTD contains several phosphorylation sites (Moss, Blackstone et al. 1993) and is reported to be the site for interaction with various proteins, which are implicated in

AMPAR trafficking and synapse anchoring (Song and Huganir 2002) (Coleman, Cai et al. 2003).

The combination of the subunits renders a great variety of AMPARs with distinct biophysical properties (Greger, Khatri et al. 2003). The GluA subunits are widely expressed throughout the mammalian brain with the following exceptions. Little or no expression of GluA1 was observed in the general motor system and in certain nuclei of the auditory, vestibular and cochlear system. Although GluA2 is the most abundantly expressed AMPAR subunit, virtually all interneurons are GluA2-free (Jonas, Racca et al. 1994). Some layers in the olfactory bulb as well as certain nuclei in the amygdala and hypothalamus are devoid of GluA3. The extent of GluA4 expression is generally weak with lowest levels in the hypothalamus (Sato, Kiyama et al. 1993)

The following regions were examined in the present study and are therefore described in more detail.

All GluA subunits are expressed within the hippocampal region (Ritter, Vazquez et al. 2002), while in pyramidal neurons GluA1/2 heteromers prevail over GluA2/3 (Anggono and Huganir 2012). GluA4 is basically absent in pyramidal neurons (Tsuzuki, Lambolez et al. 2001) (Wenthold, Petralia et al. 1996), but GluA1/4 heteromers are highly expressed in hippocampal interneurons (Fuchs, Zivkovic et al. 2007).

All four AMPAR subunits are found throughout the layers of the neocortex. Here, GluA2 is the predominant subunit and shares a very similar expression pattern with GluA3 in layers II/III, V and VI, being expressed mostly in pyramidal neurons. GluA1 is preferentially expressed in layers V and VI, mainly by non-pyramidal cells. GluA4 has the lowest expression level among AMPAR subunits in the neocortex and is preferentially expressed in astrocytes (Conti, Minelli et al. 1994).

The cerebellum displays a different distribution of GluA subunits. GluA1 is mostly expressed together with GluA2 or GluA3 in Purkinje neurons. GluA2 is found in combination with GluA4 in cerebellar granule cells, while GluA3 is additionally expressed in stellate and basket cells of the molecular layer (Hunter, Petralia et al. 1993). Bergmann glia express besides GluA1 also strongly GluA4 (Gallo, Upson et al. 1992) (Baude, Molnar et al. 1994).

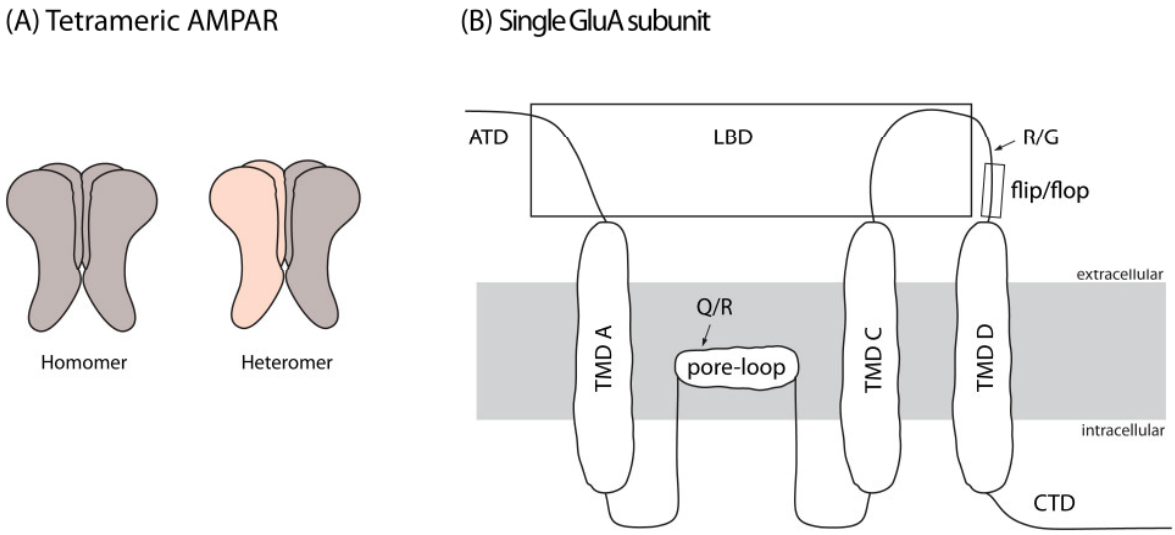

Fig. 1-2. Tetrameric AMPARs consists of four GluA subunits.
(A) Native AMPARs occur either as homomers or heteromers assembled of two different GluA subunits. (B) Each subunit contains an amino terminal domain (ATD), a ligand-binding domain (LBD) facing the extracellular space, three transmembrane domains (TMD A-C), one intramembrane pore-loop and intracellular carboxyl-terminal domain (CTD). Some GluA subunits are modified on RNA level to produce R/G, Q/R and/or flip/flop isoforms as well as subunits with short or long CTDs.

Besides the variety of AMPARs due to combinations of GluA subunits, posttranslational regulation of GluAs further increases the diversity of AMPAR receptor properties. Each GluA subunit occurs as two isoforms, termed flip and flop, created by alternative splicing of 115bp situated within the extracellular region preceeding the fourth transmembrane domain (Sommer, Keinanen et al. 1990; Koike, Tsukada et al. 2000). Flop isoforms desensitize faster than flip assemblies (Koike, Tsukada et al. 2000), while the latter is activated more efficiently by glutamate than flop isoforms (Jakowec, Yen et al. 1995). Flip isoforms are preferentially expressed in embryonic stages, with the expression of the flop isoforms increasing after birth (Monyer, Seeburg et al. 1991). Moreover the CTDs of GluA2 and GluA4 can also undergo alternative splicing, leading to short or long isoforms of these subunits (Gallo, Upson et al. 1992). The short, but not the long, isoforms contain a PDZ ligand motif (Dev, Nishimune et al. 1999) through which PDZ-domain containing proteins, such as PICK1, may modulate the localization of AMPARs (Chung, Xia et al. 2000). Furthermore GluA2 RNA is edited within the pore-loop region by Adenosine deaminase acting on RNA 2 (ADAR2). Here, the amino acid glutamine is exchanged for the positively charged arginine, which renders AMPARs that contain the edited GluA2 subunit impermeable for Ca^{2+} ions (Higuchi, Maas et al. 2000). Another site for RNA editing is located within the LBD closely to the flip/flop splice site.

In GluA2-GluA4 subunits, arginine is substituted for glycine, which leads to faster recovery rates from desensitization (Lomeli, Mosbacher et al. 1994).

1.3 AMPAR expression and function throughout brain development

Spatiotemporal variations in GluA subunit assembly and, moreover, changes at the translational level may be adaptations to the changing requirements of the evolving central neuronal system to the mature brain.
During neurogenesis, neural progenitor cells or neuroblasts give rise to neurons and glial cells by a number of asymmetrical cell divisions (Gotz and Huttner 2005). Resulting immature neurons, lacking dendrites and axons, migrate to their final destination to undergo terminal differentiation. Here, events such as synaptogenesis, axogenesis, subsequent myelination, and neural network integration govern the period of the young neuron. With ongoing maturation smaller changes occur while neurons maintain or reorganize their synaptic connections in response to activity-dependent changes in transmission.

Glutamate is present during the early phase of brain development (Root, Velazquez-Ulloa et al. 2008) and early expression of AMPARs is detectable in the CNS starting at E5 (Ni, Sullivan et al. 2007).
AMPARs are expressed in neural progenitor cells (Platel, Lacar et al. 2007); (Lidow and Wang 1995) and in glial precursors (reviewed(Nguyen, Rigo et al. 2001). Differentiating cells, which migrate out of in vitro cultivated neurospheres, express GluA1 and GluA2 subunits and costain with neuronal markers, while GluA3 colocalizes with glial markers (Jansson, Wigren et al. 2011). Functional AMPARs together with other iGluRs are present in differentiating neurons and their activation leads to inward currents and Ca^{2+} influx (Maric, Liu et al. 2000). Human neural progenitor cells express Ca^{2+} permeable AMPARs, which contain the Q/R unedited GluA2 subunit. Occurrence of this unedited GluA2 may be regulated by the low expression of ADAR2, as overexpression of this enzyme raised the proportion of Q/R edited GluA2 subunits (Whitney, Peng et al. 2008). Neuroblasts of the subventricular zone and the rostral migratory stream express functional AMPARs (Platel, Lacar et al. 2007). Inhibition of AMPARs in embryonic, hippocampal interneurons perturbs their migration (Manent, Jorquera et al. 2006). In the embryonic neocortex, glutamate release from growing axons of cortical plate cells acts on Ca^{2+} permeable AMPARs, located on tangentially orientated intermediate zone cells, and may thus control their migration (Metin, Denizot et al. 2000). In oligodendrocyte precursor cells,

AMPARs mediated signaling inhibits cell proliferation at the O2-A state and further lineage progression (Gallo, Zhou et al. 1996).
AMPAR/KAR mediated Ca^{2+} influx reduces DNA-synthesis in embryonic cortical cells (LoTurco, Owens et al. 1995) and impacts on cell-cycle progression (Martins, Linden et al. 2006), as G1 phase to S phase and S phase to M phase transitions depend strictly on levels of intracellular Ca^{2+} (Van Dolah and Ramsdell 1996; Resende, Adhikari et al. 2010).

When neurons arrive at their final destination, synaptogenesis progresses in the perinatal period and peaks at early postnatal stage (reviewed in (Risher and Eroglu 2012).
Presence of synaptic AMPARs in newly formed synapses is under debate, since these "silent synapses" do not exhibit AMPAR mediated currents at resting potentials (reviewed in (Kerchner and Nicoll 2008). However, AMPARs can be found at nascent glutamatergic synapses, but their presence is not stable yet (Groc, Gustafsson et al. 2006). In the neonatal period, postsynaptic currents mediated by NMDARs as well as AMPARs are recorded when spontaneous synaptic activity is assessed (Groc, Gustafsson et al. 2002). Additionally, presence of AMPARs during synaptogenesis does not depend on previous NMDAR activation (Rohrbough and Spitzer 1999), as neurons lacking NMDARs develop normally (Cottrell, Dube et al. 2000).
Other labs have also observed functional AMPARs in early development. Maturation of neocortical synapses is associated with a switch in subunit expression from Ca^{2+}permeable AMPARs early in development to Ca^{2+} impermeable ones containing edited GluA2 (Kumar, Bacci et al. 2002). Another study reports embryonic AMPAR mediated Ca^{2+} currents in Xenopus embryos and speculates, that AMPARs conveyed Ca^{2+} influx and therefore Ca^{2+} signaling needed for neuronal differentiation, when both the activity and the number of synapses is low (Rohrbough and Spitzer 1999).
Furthermore, the extracellular domains of GluA1 and GluA2 seem to be involved in synapse maturation. This step does not require AMPAR mediated neurotransmission. RNAi mediated silencing of AMPARs leads to an increase of presynaptic inactive synapses (Tracy, Yan et al. 2011). Another study shows, that neuroligin/neurexin contacts recruit GluA2 containing AMPARs in a cell culture model independent of preceding activity (Heine, Thoumine et al. 2008). On the other hand, activation of AMPARs/KARs inhibits the motility of axonal filopodia, the precursor of mature axons, in early development and thereby may stabilize synaptic contact (Chang and De Camilli 2001).
AMPARs contribute to synapse maturation also by increased AMPAR-mediated transmission (Wu, Malinow et al. 1996; Petralia, Esteban et al. 1999). AMPAR activation maintains dendritic spines (McKinney, Capogna et al. 1999) and reduces spine motility

(Chen, Prithviraj et al. 2009) by inhibiting actin dynamics (Fischer, Kaech et al. 2000). AMPAR overexpression increases the size of synapses and spine density (Passafaro, Nakagawa et al. 2003) as well as dendritic length (Chen, Prithviraj et al. 2009).
The last paragraphs have shown that AMPARs exert different functions depending on ontogenic stage and cell type.

The best-characterized function of AMPARs, however, is their implication in excitatory neurotransmission.
The magnitude or strength of synaptic transmission correlates with the number of AMPARs at the synapse. Insertion into and removal from synapses is accomplished in response to high and low frequency stimulation, respectively. In the case of high frequency stimulation leading to long-term potentiation, AMPARs mediate depolarization of the postsynaptic membrane, which is followed by the voltage-dependent release of the Mg^{2+} block of NMDAR. Unblocked NMDARs allow for Ca^{2+} influx, which acts downstream on kinases and phosphatases. These downstream targets affect spine remodeling as well as transcription and translation levels, all resulting in enhanced synaptic connectivity (reviewed in (Bliss and Gardner-Medwin 1973; Malinow and Malenka 2002).
AMPARs also reside at glutamatergic synapses on GABA-ergic interneurons. They are Ca^{2+} permeable and exhibit fast channel kinetics, as they tune timing and synchronization of neuronal circuit activity (reviewed in (Isaac, Ashby et al. 2007).
Besides their postsynaptic localization, AMPARs are also found presynaptically. Immunohistochemistry revealed the presence of axonal AMPARs (Ouardouz, Coderre et al. 2009) but their function is still unclear. GluA4 containing AMPARs reside on spinal axons as indicated by immunohistochemistry. AMPARs were also identified on axons of hippocampal and Purkinje neurons (Matsuda, Miura et al. 2008). They may enlarge presynaptic Ca^{2+} influx and therefore enhance synaptic transmission and neurotransmitter release (Sasaki, Matsuki et al. 2011). At presynaptic nerve terminals, AMPARs have been shown to block voltage gated Ca^{2+} channels via activation of heterotrimeric GTP-binding proteins, most likely Gβγ, therefore inhibiting neurotransmitter release (Takago, Nakamura et al. 2005).

AMPARs are also found in various types of glial cells. AMPAR mediated Ca^{2+} influx in Bergmann glia is necessary for proper innervation of Purkinje cells (Saab, Neumeyer et al. 2012). Astrocytic AMPARs contribute partly to sodium-dependent glutamate uptake and are therefore involved in the energy supply to the (presynaptic) neuron during synaptic transmission (Deitmer and Rose 2010). Microglial AMPARs regulate/mediate chemotaxis and phagocytosis in activated cells (reviewed in(Rodriguez, Sabate et al.

2013). Mature oligodendrocytes possess functional AMPARs at their soma and myelin sheats were shown to express GluA4 (reviewed in(Stys 2011).

1.4 Auxiliary subunits of AMPARs

Molecular diversity and fine-tuning of AMPAR function are further enhanced by association with auxiliary subunits.

Auxiliary subunits are proteins that interact directly and stably with ion channels and modulate their properties. Moreover, they do not form pores on their own and their presence is relevant for specific ion channel properties in vivo (Yan and Tomita 2012).

The prototypical auxiliary subunit of AMPARs has been identified by studying stargazer mice, in which cerebellar granule cells are almost devoid of AMPAR currents. Further work demonstrated, that these cells lack stargazin, a transmembrane protein that traffics AMPARs from the ER to the plasma membrane, anchors them within the synaptic density, and increases their channel conductance. Stargazin belongs to the family of transmembrane AMPAR regulatory proteins (TARPs), consisting of two subfamilies: class I TARPs (TARP-2, -3, -4,-8) and class II TARPs (TARP-5,-7). Both classes modulate the biophysical properties of AMPAR, but they differ within the PDZ ligand consensus sequence, by which they interact with synaptic scaffolding proteins such as PSD-95 and PSD-93. Class I TARPs promote AMPAR trafficking to the postsynaptic density and enhance single channel conductance by slowing deactivation and by reducing desensitization of the channel. Furthermore, class I TARPs, as well as the class II TARP TARP-7, can rescue AMPAR-mediated currents in cerebellar stargazer granule cells. Also class I TARPs enhance glutamate affinity of AMPARs, while class II TARPs either decrease (TARP-5) glutamate affinity or have no effect on this parameter (TARP-7) (Kato, Gill et al. 2010; Tomita 2010; Traynelis, Wollmuth et al. 2010; Jackson and Nicoll 2011).

Expression of TARPs is widespread within the CNS and most neurons express 2-4 different TARPs (Menuz, Kerchner et al. 2009). During CNS maturation, protein expression of all TARPs with the exception of TARP-4 increases (Tomita, Chen et al. 2003). In the adult brain, stargazin (TARP-2) and TARP-7 mRNAs are the most abundantly expressed ones among all TARP mRNAs (Fukaya, Yamazaki et al. 2005). Stargazin is the predominant isoform in the cerebellum with highest levels in Purkinje neurons and granule cells. TARP-8 is the major isoform in the hippocampus, while TARP-3 shows highest expression levels in the neocortex. Besides moderate expression in various brain regions, TARP-4 and TARP-5 are particularly expressed in the olfactory

bulb and in Bergmann glia (Tomita, Chen et al. 2003; Fukaya, Yamazaki et al. 2005; Menuz, Kerchner et al. 2009).

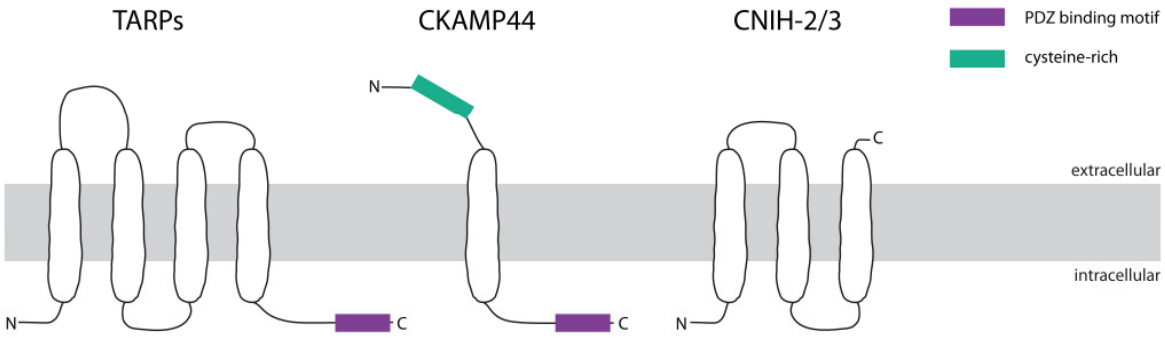

Fig. 1-4. Auxiliary subunits of the AMPAR.
Predicted membrane topology of AMPAR auxiliary subunits. TARPs contain four transmembrane domains, CKAMP44 possesses one, both subunits comprise a PDZ ligand motif. Additionally, CKAMP44 has a N-terminal cystine-rich region. CNIH-2/3 have three predicted transmembrane domains and no PDZ consensus site.

With progress in the field of proteomic research and the isolation of native complexes, more auxiliary subunits have been identified. After the characterization of CNIH-2and CNIH-3 as constituents of the native AMPAR complex, which will be introduced below, another protein, CKAMP44, was identified that integrates in native AMPAR complexes.
The extracellular N-terminus of CKAMP44 endows several cysteines forming a cys-knot, which are putative interaction sites for the AMPAR. Besides a single transmembrane domain, CKAMP44 also contains a PDZ ligand domain. It is expressed in many brain regions and most prominently in the dentate gyrus of the hippocampus. It acts on AMPARs by slowing deactivation and increasing glutamate affinity in a similar manner as TARPs, but in contrast increases AMPAR desensitization by slowing their recovery from desensitization. AMPARs carrying mutations that favor the stability of the close-cleft conformation of the ligand binding domain exhibit similar functional properties, therefore CKAMP44 is hypothesized to stabilize the close-cleft conformation of the AMPAR. CKAMP44 mediated reduction of paired-pulse facilitation hints at its implication in short-term plasticity (von Engelhardt, Mack et al. 2010).
Further and more sophisticated proteomic analysis exposed 21 new AMPAR complex constituents. Native AMPAR complexes were solubilized from brain tissue using mild, intermediate, and stringent detergent conditions leading to differentially preserved macromolecular complexes (Schwenk, Harmel et al. 2012).

1.5 Cornichon Proteins

Cornichons were first described in Drosophila as crucial components of the early axial determination in oogenesis (Roth, Neuman-Silberberg et al. 1995).
Further studies have shown that these proteins belong to a highly conserved family of ER cargo transporters. The yeast ortholog Erv14p promotes intracellular transport of the transmembrane protein Axl2p, which is required for bud-site selection (Powers and Barlowe 1998).

In metazoans, the cornichon orthologs facilitate secretion of growth factors of the EGF superfamily. One growth factor out of this family, TGF-alpha, is exported by CNIH-1 in human cell lines (Castro, Piscopo et al. 2007). In Drosophila, correct secretion of the TGF-alpha-related Gurken depends on its precisely timed and localized cornichon-mediated ER export at the future dorsal site within the developing egg. Locally concentrated Gurken then activates the Drosophila EGF receptor (DER/torpedo) and further establishes dorso/ventral patterning of the egg chamber (Roth, Neuman-Silberberg et al. 1995; Bokel, Dass et al. 2006) In early chicken oogenesis, cornichon is distinctly expressed in certain rhombomeres of the neurosphere tissue and fascilitates secretion of the Heparin binding-epidermal growth factor (HB-EGF). This growth factor serves as a ligand for the ErbB4 receptor and by activation of this receptor guides the migration of neural crest cells (Hoshino, Uchida et al. 2007).
In 2009, mammalian CNIH-2 and CNIH-3 were surprisingly identified to be integral parts of the native AMPAR complex extracted from whole rat brain. Upon heterologous co-expression, CNIH-2 increased GluA1 surface expression and slowed deactivation and desensitization of the AMPAR (Schwenk, Harmel et al. 2009).

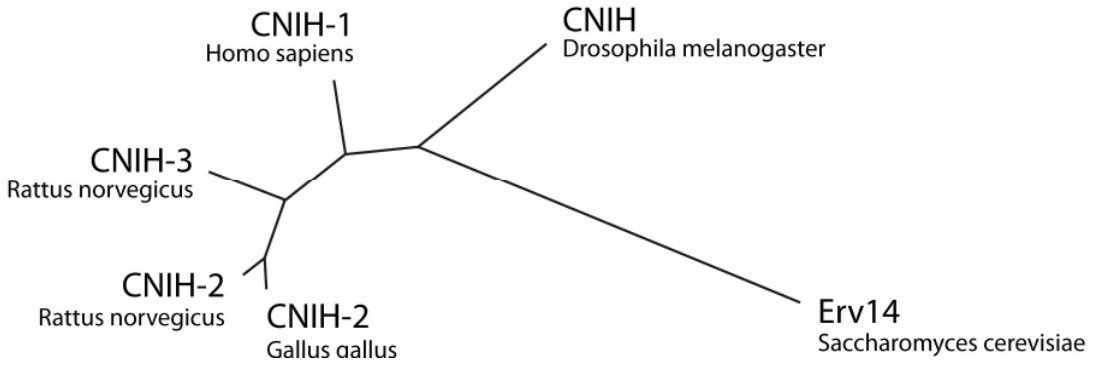

Fig. 1-5. Schematic phylogenetic tree of the highly conserved cornichon orthologues.
The unrooted phylogenetic tree depicts the relationship based on sequence homology of cornichon orthologs from several species according to the literature.

However, Shi et al. proposed an ER export function for CNIH-2 in neurons as they failed to detect CNIH-2 at neuronal cell surfaces and also did not find CNIH-2 to modulate AMPAR kinetics in cerebellar granule cells (Shi, Suh et al. 2010). Another study found CNIH-2 to segregate in synaptosomal fractions, together with TARPs and GluA1 (Kato, Gill et al. 2010). Heterologously expressed AMPARs together with TARP-8, the predominant TARP isoform in hippocampal pyramidal neurons, show a gating phenomenon termed resensitization. In hippocampal neurons, however, AMPARs do not resensitize, which was interpreted to be due to the presence of CNIH-2 in native surface complexes, as CNIH-2 also overrides the TARP-8 mediated gating effect of resensitization in heterologous cells (Kato, Gill et al. 2010). Besides affecting the biophysical characteristics of AMPARs synergistically with TARPs (Gill, Kato et al. 2012), CNIH-2 regulates TARP/AMPAR stoichiometry by determining the number of TARPs being associated in AMPAR complexes in hippocampal neurons, favoring a low TARP/AMPAR stoichiometry (Gill, Kato et al. 2011).

A recently published study on the impact of CNIH-2/3 gene deletion on AMPARs demonstrated a severe reduction of AMPAR mediated synaptic transmission in the hippocampus. Loss of CNIH-2/3 resulted in reduced levels of surface GluA1/2 heteromers (Herring, Shi et al. 2013). Considering the importance of available, extrasynaptic pools of AMPARs for LTP (Granger, Shi et al. 2013), the reduction of these in hippocampal neurons predominantly present AMPAR heteromers (Wenthold, Petralia et al. 1996) may lead to profound impairments of LTP.

2.1 Objectives

Cornichon proteins had been described in two different contexts: Originally, they were identified as cargo exporters of EGF-like growth factors in several species. More recently, they were also discovered to be constituents of native AMPAR complexes in brain. To shed more light on the physiological significance of cornichons, the present study was designed to address the following questions:

(1) As CNIH-2/3 increase the surface population of AMPARs and modulate the biophysical properties of the AMPAR in heterologous expression systems (Schwenk, 2009), it should be clarified whether this holds also true for neuronal cells and, if so, which molecular mechanisms underlie the increase in AMPAR numbers at the plasma membrane.
(2) As the ontogenic expression pattern of a protein can hint at its physiological role, the mRNA and protein expression levels of CNIH-2/3 should be characterized in comparison with the ones of the pore-forming AMPAR subunits.

2. Material and methods

2.1 Material

2.1.1 Laboratory equipment

Agarose gel electrophoresis equipment (Horizon 58)	Gibco
Balance	VWR International, Sartorius
Centrifuges	
Biofuge 13; Megafuge 1.0	Heraeus
Centrifuge 5417R; 5424 R	Eppendorf
Optima MAX-XP ultracentrifuge	Beckmann Coulter
BioPhotometer Plus	Eppendorf
Freezer (-80°C; -20°C & 4°C)	Thermo Scientific; Liebherr
Gel documentation system for Agarose gels (UV Solo TS)	Biometra
Genetic Analyzer ABI PRISM 310	Applied Biosystems
Hybridization oven (OV3)	Biometra
Incubator (Heraeus BBD 6220)	Thermo Scientific
Luminometer (GloMax 20/20)	Promega
Microscope (Axiovert 100)	Carl Zeiss Microimaging GmbH
pH meter (Seven easy)	Mettler Toledo
Pipettes, adjustable	Eppendorf
Power supply	Bio-Rad Laboratories
Protein electrophoresis system (Mini PROTEAN Tetra cell)	Bio-Rad Laboratories
Shaking incubator (GFL 3031)	VWR International
Sonifier 250	Branson
Thermocycler (Mastercycler Gradient)	Eppendorf
Thermomixer	Eppendorf
Vortex	VWR International
Western blot imaging and detection (Fusion Fx)	Vilber Lourmat

Water bath	VWR International

2.1.2 Consumables

Cell culture flasks (250 ml)	Greiner Bio-One
Cover glasses for microscopy (Ø 13mm)	Menzel (VWR international)
Cuvettes, polystyrene	VWR International
Disposable gloves	Ansell
Dounce tissue grinder (1 ml; 10ml)	Wheaton
Gel blotting paper	Whatman
Immobilon-P Transfer Membrane	Millipore
Petri dishes (Ø 34 mm)	Greiner Bio-One
Pipette tips (0.1 -10µl)	Gilson
Pipette tips (1 - 20 µl; 1 - 200 µl; 101 - 1000 µl)	Starlab
Test plates (24-well)	Greiner Bio-One
Tubes (1.5 ml; 15ml, 50ml)	Eppendorf; Falcon BD
Tubes for ultracentrifuge (1.5 ml)	Beckmann

2.1.3 Chemicals, reagents and media

All reagents were purchased from Sigma unless otherwise stated.

10x Trypsin/EDTA	Invitrogen
Acrylamide / Bis solution 30%	Bio-Rad Laboratories
Agarose	Invitrogen
Alkaline phosphatase	Roche
BCA Protein Assay Kit	Thermo Scientific
BCIP (5-Brom-4-Chlor-3-Indolylphosphat)/ /NBT (nitro-blue tetrazolium chloride)	Roche
BigDye Terminator v1.1 Cycle Sequencing Kit	Applied Biosystems
Blocking Reagent	Roche
Bovine serum albumin (BSA) standard	Pierce
Buffer for restriction endonucleases	Fermentas
ComlplexioLyte-48	Logopharm GmbH
ComplexioLyte-82	Logopharm GmbH
Denhardt´s solution (50x)	Invitrogen

Deoxynucleotide Mix ("dNTPs")	Stratagene
Dextransulfat	Pharmacia Biotech
DIG RNA Labeling Mix 10x	Roche
Dithiothreitol	Fluka
DMEM / F12	Invitrogen
DMEM + Glutamax (4.5g glucose/l)	Invitrogen
DNA molecular weight marker (1 kbp, 100 bp)	Fermentas
Dry milk, nonfat	Saliter
Dynabeads mRNA DIRECT Kit	Invitrogen
Dynabeads Protein A (30 mg/ml)	Invitrogen
ECL Prime Western Blotting Detection System	GE Healthcare
Escherichia coli Xl 1 Blue	Stratagene
Ethanol	Roth
Fetal calf serum (FCS)	Biochrom AG
FuGene HD Transfection Reagent	Roche
Gel loading buffer (6x)	Ambion
Glutamax	Invitrogen
Glycerin	Roth
Hering sperm DNA 10 mg/ml	Invitrogen
Kaiser´s glycerol gelatin	VWR International
Potassium phosphate monobasic (KH_2HPO_4)	Fluka
Leupeptin	Roth
Lipofectamine 2000 Reagent	Invitrogen
Luria Broth Base ("LB")	MP Biomedicals
Loading Dye	Ambion
Maleic Acid	Roth
Sodium Chloride (NaCl)	Roth
Normal goat serum (NGS)	Millipore
NucleoSpin Extract II	Macherey-Nagel
NucleoSpin Plasmid QuickPure	Macherey Nagel
Oligonucleotides ("primers")	biomers.net
Paraformaldehyde	Electron Microscopy Sciences
Penicillin / streptomycin	Biochrom AG
Plasmid DNA Purification	Macherey-Nagel
Pepstatin A	Roth
Precision Plus Protein Standards All Blue	Bio-Rad Laboratories
Proteinase K 20 mg/ml	Roche
Pwo-DNA-Polymerase 10x buffer	Stratagene

Pwo-Ultra-Hotstart-DNA-Polymerase 2.5 U/µl	Stratagene
Restriction endonucleases	Fermentas
RNA ladder (0.24 - 9.5 kb)	Invitrogen
SDS (sodium dodecyl sulfate)	Roth
SuperSignal ELISA Femto Maximum Sensitivity Substrate	Thermo Scientific
SyberSafe	Invitrogen
Triethanolamine	Fluka
T3 RNA-Polymerase 20 U/µl	Ambion
T4 DNA ligase	Roche
T7 RNA-Polymerase 20 U/µl	Ambion
Yeast t-RNA	Invitrogen

2.1.4 Vectors

pBluescript II SK (-); ampicillin	Stratagene
pcDNA3.1+; ampicillin	Invitrogen
pEGFP-C2; kanamycin	BD Biosciences-Clonetech

2.1.4 Buffers and solutions

10x PBS

Na_2HPO_4	8,1 mM
KH_2HPO_4	1,6 mM
NaCl	150 mM
KCL	2,7 mM
pH 7,4	

1x TAE

Tris/HCl (pH = 8.0)	40 mM
Acetate	20 mM
EDTA	1 mM

10x MOPS running buffer

MOPS 1M (pH = 7.0)	10 ml
Na-Acetate 3M (pH = 4.8)	0.83 ml
EDTA 0.5M (pH = 8.0)	1 ml
Sigma H_2O	ad 50 ml

RNA premix

10x MOPS running buffer	0.129 ml
Formaldehyde 37%	0.226 ml
Formamide	0.645 ml
Sigma H_2O	ad 1 ml

4x separating gel buffer

Tris/HCl (ph = 8.8)	1.5 M
SDS	0.4 %

4x stacking gel buffer

Tris/HCl (pH = 6.8)	0.5 M
SDS	0.4 %

Tissue homogenization buffer	
Sucrose	0.32 M
Tris-HCl (pH = 7.4)	0.01 M
EDTA (pH = 8.0)	0.01 M
iodacetamide	0.01 M

Resuspension buffer	
Tris-HCl (ph = 7.4)	0.02 M
EDTA (pH = 8.0)	0.01 M
iodacetamide	0.01 M

10x SDS running buffer	
Tris/HCl	0.25 M
Glycine	1.92 M
	0.192 M
SDS	1 %

1x blotting buffer	
Tris/HCl	0.025 M
Glycine	
Ethanol	20 %

5x Laemmli buffer	
Tris/HCl (pH = 6.8)	0.312.5 M
Glycerin	50 %
SDS	10 %
DTT	0.5 M
Bromphenolblue	0.05 %

20x SSC buffer	
NaCl	3 M
Sodium citrate	0.3 M
pH = 7	

Hybridization buffer	
Formamide	50 %
SSC	5x
Denhardt´s solution	5x
Yeast t-RNA	250µg/ml

Maleic acid buffer (MAB)	
Maleic acid	0.1 M
NaCl	0.15 M
pH = 7.5	

Alkaline phosphatase (AP) buffer	
Tris/HCl (pH = 9.0)	0.1 M
NaCl	0.1 M
$MgCl_2$	0.05 M

10x TBS	
Tris/HCl	0.5 M
NaCl	1.5 M
pH = 7.4	

Neurobasal (NB)/FCS

NB/B27

2.1.5 Antibodies

Anti-Digoxigenin-AP Fab fragments from sheep	Roche
Rabbit anti-CNIH-2	

(Epitope: GNPARARERLKNIERIC)	(Hoshino, Uchida et al. 2007)
Guinea pig anti-CNIH-2	
(Epitope: DELRTDFKNPIDQGNPARARERLKNIERIC)	Charles River
Rabbit anti-HB-EGF (H-88)	Santa Cruz Biotechnology
Goat anti-rabbit IgG (HRP coupled)	Santa Cruz Biotechnology
Goat anti-mouse IgG (HRP coupled)	Santa Cruz Biotechnology
Goat anti-guinea pig IgG (HRP coupled)	Santa Cruz Biotechnology
Mouse anti-HA IgG (monoclonal)	Santa Cruz Biotechnology
Rabbit anti-GluA1 (AB1504)	Millipore
Rabbit anti-GluA2 (MAB397)	Millipore
Mouse anti-GluA2 (75-002)	NeuroMab
Rabbit anti-GluA2/3 (07-598)	Millipore
Rabbit anti-GluA4 (AB1508)	Millipore
Rabbit anti-Cacng2 (07-577)	Millipore
Rabbit anti-beta actin (ab8227)	Abcam
Mouse anti-GM130 (610822)	BD Transduction Laboratories

2.1 Molecular biology

2.1.1 Extraction of nucleic acids

Total RNA was extracted from cultured HeLa cells, grown to 80% confluency in a T75 culture flask, with Dynabeads mRNA DIRECT kit from Invitrogen. Plasmid DNA was extracted from Bacteria overnight cultures with NucleoSpin Plasmid QuickPure or Plasmid DNA Purification, both from Macherey-Nagel. Extraction and purification of DNA from agarose gels was performed using the NucleoSpin Extract II Kit from Macherey-Nagel. All experiments were accomplished according to the manufacturer´s specifications.

2.1.2 Complementary DNA synthesis

Complementary DNA (cDNA) was generated by reverse transcriptase, an enzyme that transcribes RNA to DNA. CDNA was synthesized using SuperScript II Reverse Transcriptase for RT-PCR Kit from Invitrogen.

4µl of RNA samples were mixed and incubated with 1µl of primer (1:1 mix of oligoT and hexanucleotides) at 72°C for 2min to allow for annealing of primers.

Master mix:	
5x buffer	2 µl
DTT (100 mM)	1 µl
RNAse inhibitor	0.5 µl
dNIPs (10 mM)	1 µl
SuperScript II	0.7 µl

Master mix was then added and all components were incubated at 42°C for 2 hours to allow for transcription. Reaction was terminated by an incubation step at 75°C for 10 min, to denature the transcriptase enzyme. The resulting cDNA was diluted with 40µl of Sigma water and stored at -20°C.

2.1.3 Polymerase chain reaction

Polymerase chain reactions (PCR) were performed to amplify specific regions of DNA.
The standard PCR set-up contained:

cDNA	0.5µl
Pwo Polymerase	0.25µl
10x buffer	2.5µl
forward primer (10µM)	1.5µl
reverse primer (10µM)	1.5µl
dNTPs (10mM)	0.5µl
Sigma H_2O	ad 25 µl

Cycling conditions were as follows:

1	initial denaturing step	94°C	2min
2	denaturing	94°C	30s
3	primer annealing	calculated	30s
4	extension (500bp/min)	72°C	dependent on length DNA fragment to be amplified
5	final extension step	72°C	2min
6	cooling	4°C	∞

Steps 2, 3 and 4 were repeated 30 times.

2.1.4 Synthesis of riboprobes

RNA riboprobes for in situ hybridization were generated as run-off transcripts from plasmids containing either CNIH-2 or CNIH-3, both in antisense (T7) and sense (T3) direction.
CNIH-2 and CNIH-3 rat cDNAs were cloned into pBluescript II reverse vector (Stratagene) using EcoRI or HindIII and XhoI restriction sites, respectively. Resulting plasmids were linearized with the restriction enzyme Acc65I for the synthesis of sense probes and with BamHI (CNIH-2) or EcoRI (CNIH-3) for the synthesis of antisense probes.
Riboprobes were generated by in vitro transcription with T7 or T3 RNA polymerase (Ambion) and were labeled with DIG (Roche) according to the manufacturer's manual. Labeling efficiencies were determined using DIG quantification and control test strips (Roche). Specificity of riboprobes was tested by in situ hybridization using HeLa cells transduced with each of the four cornichon rat homologues.

2.1.5 Agarose Gel Electrophoresis

DNA and RNA molecules were separated according to their sizes by agarose gel electrophoresis.
DNA was mixed with 6x loading dye (Ambion) and loaded onto a 1% agarose gel (containing 4 µl sybersafe/ 100 ml) to allow for visualization of DNA. The gel was run in 1x TAE buffer, for 20-30 min at 120 Volt. The molecular weight marker GeneRuler DNA ladder (Thermo Scientific) was used for comparison to determine DNA fragment sizes.
1 µl of RNA sample as well as 3 µl of RNA ladder (Invitrogen) were denatured each in 10 µl of RNA premix at 65°C for 10 min and then cooled on ice, in order to reduce secondary structures prior to gel electrophoresis. 1 µl of loading buffer (Ambion) was added to each sample and then loaded onto a 0.75% agarose gel (containing 10x MOPS buffer, 12.3 M formaldehyde, 0.5 µl ethidium bromide/ 100 ml). RNA molecules were separated for 15 min at 140 Volt in 1x MOPS running buffer supplied with 0.5 µl ethidium bromide/ 100 ml. The UV Solo TS imager system (Biometra) was used for documentation.

2.1.6 Enzymatic DNA digestion

DNA fragments were digested with restriction endonucleases for either analytical purposes or for subsequent DNA cloning.
1 µg of plasmid DNA was incubated with 5 units of restriction enzyme in the appropriate buffer (Fermentas) at 37°C for 1 hour. Digested vectors were dephosphorylated by addition of 1µl of alkaline phosphatase at 37°C for 15min to prevent re-ligation.

2.1.7 Ligation of DNA fragments

Digested and purified PCR products or DNA fragments were subcloned into target vectors using T4 Ligase (Roche).

ligase reaction mixture	
1 µg of digested vector	1 µl
1 µg of digested fragment	1 µl
10x ligation buffer	2 µl
T4 DNA ligase (5 U/µl)	1 µl
Sigma H_2O	ad 10 µl

To control for re-ligation of the vector, water instead of the insert was added to the ligation mixture. The mixture was incubated at 16°C over night.

2.1.8 Transformation of DNA

For amplification of ligated DNA fragments, plasmids were introduced into bacteria.
70µl of chemocompetent bacteria (Escherichia coli, XL1 blue, Stratagene) were thawn on ice and 3µl of the ligation product were added. Suspension was incubated for 20 min on ice prior to heat shock at 42°C for 90s. Suspension was then again placed on ice for 10min, 500µl of LB-Medium were added and plated on an agar plate containing the appropriate selection antibiotics for the plasmid and incubated at 37°C over night.

2.1.9 Sequencing

DNA sequencing was performed using the dideoxy nucleotide chain-termination method with dye terminator labeling of purified plasmids. Experiments were performed with the BigDye Terminator v1.1 Cycle Sequencing Kit (Applied Biosystems).
Universal forward and reverse primers as well as specific primers for inserted DNA fragments were used.
The sequencing reaction contained:

template DNA (500ng)	0.5 µl
primer (5 pM)	1 µl
Big Dye	2 µl
Sigma H2O	ad 10 µl

Sequences were analyzed on ABI Prism Genetic Analyzer automatic sequencer (Applied Biosystems).

2.2 Cell biology

2.2.1 Cell culture

All cell lines were maintained at 37°C and 5% CO2. For heterologous expression assays, HeLa (DSMZ) and Opossum kidney (American Type Culture Collection) cells were used. HeLa and Opossum kidney (OK) cells were grown in Dulbecco´s modified eagle medium (DMEM) and DMEM-F12, respectively. Both media were supplemented with 10% FCS, 1% penicillin/streptomycin (P/S). For HeLa culture medium, 1x Glutamax was added. Cells were split regularly up to 60 passages before new stocks were thawed in 1/20 and 1/30 ratios for HeLa and OK cells, respectively. Cells were split at 90-100 % confluency using 1x trypsin for HeLa and 2x trypsin for OK cells. Culture medium was added after trypsin treatment and cells were pelleted at 1000rpm for 2 min.

2.2.2 Primary cultures of hippocampal neurons

Primary cultures of rat hippocampal neurons were prepared from timed-pregnant (E18) Wistar rats (Janvier) as described previously (Kaech & Banker, 2007).
The entire hippocampus was isolated from brains of rat pups and collected in chilled HBSS buffer. Tissue was incubated in 0.05% trypsin at 37°C for 10min. After two washing

steps with DMEM supplied with 10% FCS to inactivate trypsin and one with Neurobasal medium/FCS (containing 10% FCS, 1% Na-pyruvate, 1% glutamax, 1% P/S and1% Fungizone; all Invitrogen), cells were dissociated using fire polished Pasteur pipettes and plated in a 24-well plate at a density of 50 000 cells/ well on poly-D-lysine coated coverslips. Neurons were allowed to settle for 4 hours before being transferred in glia-conditioned Neurobasal medium containing 2% B27, 1% Na-pyruvate, 1% glutamax, 1% P/S and1% Fungizone.

2.2.3 Transfections

HeLa and OK cells were grown to 80-90 % confluency before transfection. Plasmid DNA transfections into HeLa cells were performed with FuGENE HD Transfection reagent (Roche) and into OK cells with LipofectAMINE (Invitrogen) according to the supplier´s instructions.

2.2.4 Viral transduction of neurons

Primary hippocampal neurons were transduced with CNIH-2 by high-titer lentiviral preparations at days 12–14 in vitro (DIV 12–14).

2.2.5 Immunocytochemistry

Subcellular localization as well as expression levels of proteins were visualized by immunofluorescent analysis of Hela, OK and primary neuronal cells.
At 24 – 48 hours post transfection, Hela and OK cells were fixed in 4% paraformaldehyde (PFA) in PBS, and neurons in 4% PFA in PBS containing 1.3 M sucrose, both at 4°C for 10 min. Pretreatment with 10% normal goat serum in PBS with 0.04% Triton X-100 (PBS-T) was performed for 1 hour at room temperature (RT), in order to prevent unspecific antibody-binding. Cells were then incubated with the respective primary antibodies in 2% NGS in PBS-T at RT for 1 hour. After washing with PBS, cells were incubated with secondary antibodies conjugated to cy-2, cy-3 or cy-5 (1:250 in 10% NGS in PBS-T, Dianova). Cells were mounted in fluorsave reagent (Calbiochem).
Cells were imaged with a confocal laser scanning microscope (LSM510, Zeiss) using the following excitation wavelengths and filter settings. EGFP, cy-2: Ar-laser (488 nm), BP505–530 nm; cy-3: HeNe-laser (543 nm), LP560 nm; cy-5: HeNe-laser (633 nm), BP690–750 nm.

2.2.6 Preparation of cryosections

Brains from E18, P2 and P10 rats were subjected to immersion fixation in 4% paraformaldehyde in PBS, at 4°C over night. P21 and adult (>P42) Wistar rats were anesthetized and perfused transcardially with 0.9% saline followed by fixative solution. P21 and adult brains were post-fixed at 4°C for 6 hours. All brains were dehydrated in PBS containing 20% sucrose at 4°C over night and stored at -80°C. Cryosections of 20-25µm thickness were prepared in sagittal orientation

2.2.6 Immunohistochemistry

For immunohistology, cryosections on slides were washed with PBS containing 0.8% Triton-X (PBS-T), blocked and permeabilized for 45min in PBS -T supplied with 2% normal goat serum and incubated with rabbit anti-CNIH-2 (1:250 in PBS-T with 2% NGS) over night at 4°C. Tissue sections were washed 3x 10min with PBS-T before incubation with Cy3- conjugated goat anti-rabbit antibody in 1x PBS-T with 2% NGS for 90 min. After repeated washing with PBS, slides were embedded in fluorsave reagent (Calbiochem). Tissue sections were imaged with a Zeiss Axio Observer Z1 microscope.

2.2.7 In situ hybridization

For detection of mRNA, a standard in situ hybridization protocol was used. Brain tissue sections from indicated time points in development were assayed in one experimental run to be able to compare signal intensities.
Tissue sections were pretreated with 0.2M HCl for 10 minutes, digested with proteinase K (Roche) at 37° for 5 min and acetylated (0.1M triethanolamine, 0.25% acetic anhydride, pH 8) before incubation with 0.5ng/ml riboprobes in hybridization buffer at 57°C and 60°C over night for CNIH-2 and CNIH-3, respectively. Sections were then washed twice with 50% formamide and 2x SSC at hybridization temperatures for 1 h, before rebuffering them in MAB. After blocking them with Roche blocking reagent (1% in MAB) for 1 hour, they were finally incubated with alkaline phosphatase (AP) conjugated anti-DIG Fab fragments antibody (1:2000 in blocking solution; Roche) at 4°C over night. Sections were washed 3x 20min with 1x MAB and 2x 10min with AP buffer. DIG-label was visualized by chromogenic detection of AP-activity using 5-bromo-4-chloro-3-

indolyl-phosphate/nitro blue tetrazolium (BCIP/NBT 1:50, Roche) in AP buffer. Sections were mounted in Kaiser´s glycerol gelatine (VWR International).

2.2.8 Quantification of cell surface expression of proteins

The following luminometer-based assay was performed to quantify levels of protein expressed at the plasma membrane.
Transfected HeLa cells were grown to 100% confluency in 34 mm dishes, fixed in 4% PFA in PBS for 20 min and pre-treated with 10% NGS in PBS for 1 hour before incubation with a primary mouse anti-HA antibody (1:100, Santa Cruz) or rabbit anti-HB-EGF-antibody (1:100, Santa Cruz) for 1 hour. After brief washing in PBS, cells were incubated with either goat anti-mouse or goat anti-rabbit secondary antibody conjugated to horseradish peroxidase (1:5000 in 10% NGS in PBS, Santa Cruz). SuperSignal ELISA Femto Maximum Sensitivity Substrate (Thermo Scientific) was used to detect enzymatic turnover, which was quantified in a GloMax 20/20 n luminometry system (Promega). All experiments were conducted in the absence of detergents and at room temperature. Test and control dishes were always processed in parallel.

2.3 Biochemistry

2.3.1 Preparation of membrane proteins

Isolated brains from developmental stages E18, P2, P10, P21, and from adult rats were homogenized with dounce tissue grinders (Wheaton) in ice-cold homogenization buffer All buffers used contained freshly added protease inhibitors (PI-mix: aprotinin, pepstatin A and leupeptin, 0.1mg/ml).
Cell debris and nuclei were removed by centrifugation at 1000g for 4min at 4°C. The supernatant was ultracentrifuged at 125,000g for 30 min at 4°C, the resulting pellet containing the crude membrane fraction was mixed with resuspension buffer.
Protein concentration was determined by the BCA protein assay kit (Thermo Scientific) using bovine serum albumin (Pierce) as a standard. Samples for immunoprecipitation assays were solubilized in ComplexioLyte buffer CL-48 (Logopharm GmbH) at 1mg/ml for 30min at 4°C. Membrane proteins used for developmental expression analysis were solubilized with ComplexioLyte buffer CL-82 (Logopharm GmbH) at 1mg/ml for 30min at 4°C before addition of Laemmli buffer.

2.3.2 Immunoprecipitation

Immunoprecipitation assays were performed to pull down target proteins and co-purify proteins, that interact with the target protein.
Solubilisates (1.5 ml) were incubated with 15-30 µg immobilized antibodies at 4°C for 3 hours on a rotating wheel. The following mixture of antibodies was used: 30% of anti-GluA1 (AB1504, Millipore), 40% of anti-GluA2 (AB1768, Millipore; 75-002, NeuroMab), 25% of anti-GluA2/3 (07-598, Millipore) and 5% of anti-GluA4 (AB1508, Millipore). After 4 washing steps with 0.1% ComplexioLyte buffer CL-48, bound proteins were eluted with 1x Laemmli buffer at 37°C for 10min and 0.1M DTT was added after elution.

2.3.3 SDS polyacrylamide gel electrophoresis

Proteins were separated by their molecular weights under denaturing conditions in a sodium dodecyl sulfate polyacrylamide gel electrophoresis (SDS-PAGE).
8 ml of 10% separating gel were poured into a mini PROTEAN handcast apparatus (BioRad), allowed for polymerization, and covered with 2.5 ml of 4% stacking gel.
Protein samples were denatured in Laemmli buffer at 37°C for 10 min before loading onto gels. To estimate the molecular weight of the sample proteins, Precision Plus Protein Standards All Blue (BioRad) was used for comparison. Proteins were separated at 100 V for 1-2 hours.

2.3.4 Western blotting

Proteins previously separated by SDS-PAGE were transferred onto a membrane and detected with antibodies directed against respective target proteins.
Gel-separated proteins were transferred in blotting buffer onto a PVDF membrane (Millipore). Blotting conditions were 2hrs at 50 V using a tank blot apparatus (BioRad).
The blot was then cut horizontally into different molecular weight ranges, blocked for 1 hour with 1x Tris-buffered saline (TBS) containing 1% tween-20 (TBS-T) and 5% nonfat powdered milk and incubated over night at 4°C with: 0.5µg/ml of anti-TARP-γ2/3/8 (07-577, Upstate), anti-GluA1 (AB1504, Millipore), anti-GluA2 (75-002, NeuroMab, detection of IP-blots: MAB397, Millipore), anti-GluA2/3 (07-598, Millipore), 1µg/ml of anti-GluA4 (AB1508, Millipore) and anti-CNIH-2/3 (1:1000, (Hoshino, Uchida et al. 2007)in TBS-T and 2% nonfat powdered milk. Primary antibodies were recognized by goat anti-mouse or anti-rabbit secondary antibodies conjugated to horseradish peroxidase (Santa Cruz, 1:15000 in TBS-T with 5% nonfat powdered milk). Blots were finally developed with ECL

prime Western Blotting Detection System (GE Healthcare) and results were recorded using Fusion Fx (Vilber Lourmat).

2.4 Electrophysiology

Experiments were conducted by Gerd Zolles and Henrike Berkefeld. See (Harmel, Cokic et al. 2012) for Materials and Methods.

2.5 Statistical analysis

Data are given as mean ± standard error of mean (SEM) unless otherwise stated. For assessing statistically significant differences, either two-tailed unpaired Student's t-test or one way ANOVA were used.

3. Results

3.1 The ER cargo exporter CNIH-2 acts as an AMPAR auxiliary subunit

A proteomic analysis has recently identified the cornichon homologues CNIH-2 and CNIH-3 as constituents of native AMPAR complexes in rodent CNS.. Initial functional experiments postulated a novel role for this protein family, up to this point best known for their role as cargo exporters for growth factors of the EGF superfamily. Thus, in heterologous cells, the co-expression of CNIH-2 did not only lead to a significant increase in the AMPAR surface population but also modified its biophysical properties (Schwenk, Harmel et al. 2009)
In a follow-up study, we wanted to investigate the role of CNIH-2 as a putative AMPAR auxiliary subunit in more detail.

First, the preferred subcellular localization of CNIH-2 was examined upon heterologous expression in HeLa cells and upon overexpression in neurons using immunocytochemistry (Fig. 3-1).

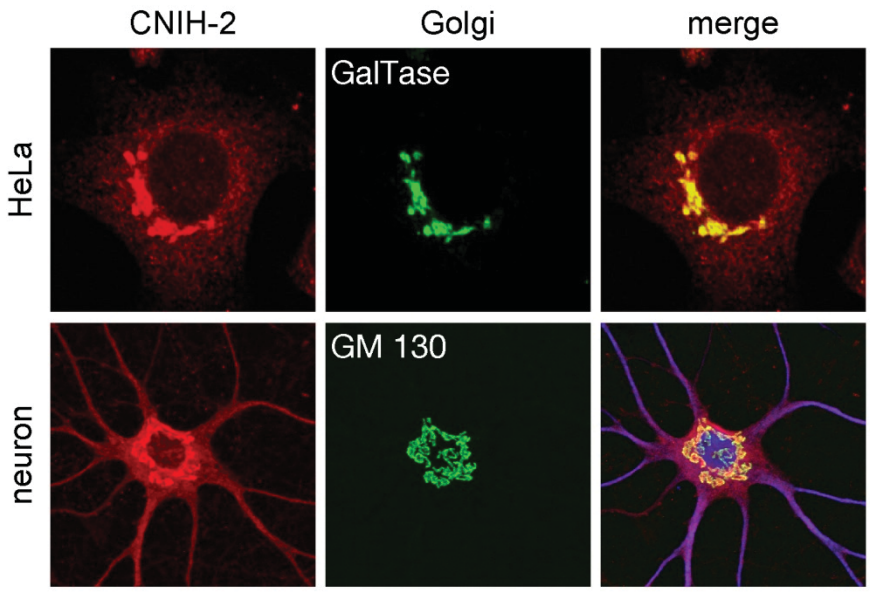

Fig. 3-1. Subcellular distribution of CNIH-2 in heterologous and primary cells.
Representative confocal images of transiently expressed CNIH-2, that colocalizes with Golgi markers, such as GalTase in HeLa cells (upper panel) and with GM130 in primary neurons (lower panel). Modified from (Harmel, Cokic et al. 2012).

Both in HeLa cells and primary hippocampal neurons, CNIH-2 immunoreactivity was predominantly present at perinuclear structures, corresponding to the endoplasmic reticulum (ER) and Golgi complex, as proven by morphology and co-localization with Golgi-specific marker proteins such as beta-1,4-galactosyltransferase (GalTase) and GM130, respectively.

The common ancestral role of cornichon orthologs is to promote ER export of cargo proteins in a COPII-dependent manner. We therefore asked whether this export mechanism applies also for AMPARs, as they had been shown to increase in surface expression upon co-expression of CNIH-2 (Schwenk, Harmel et al. 2009)

Opossum kidney (OK) cells were chosen for the next experiment, since their large cytoplasm-to-nucleus ratio allows for good identification of subcellular structures. An OK cell line stably expressing CNIH-2 was used in further experiments that required heterologous co-expression of multiple proteins.

Anterograde ER-to-Golgi trafficking was inhibited (Fig. 3-2) by co-expression of Sar1 H79G (Sar1 mutant). Sar1 is a small Ras-like GTPase centrally involved in COPII-coated vesicle formation. Its dominant-negative mutant H79G cannot hydrolyze GTP and therefore blocks COPII budding (Szul and Sztul 2011). While coexpression of Sar1 WT did not affect the accumulation of CNIH-2 in the Golgi complex, co-expression of the mutant led to a retention of CNIH-2 within the ER, as can be judged by the network-like pattern of its immunofluorescence (Fig. 3-2; lower panel).

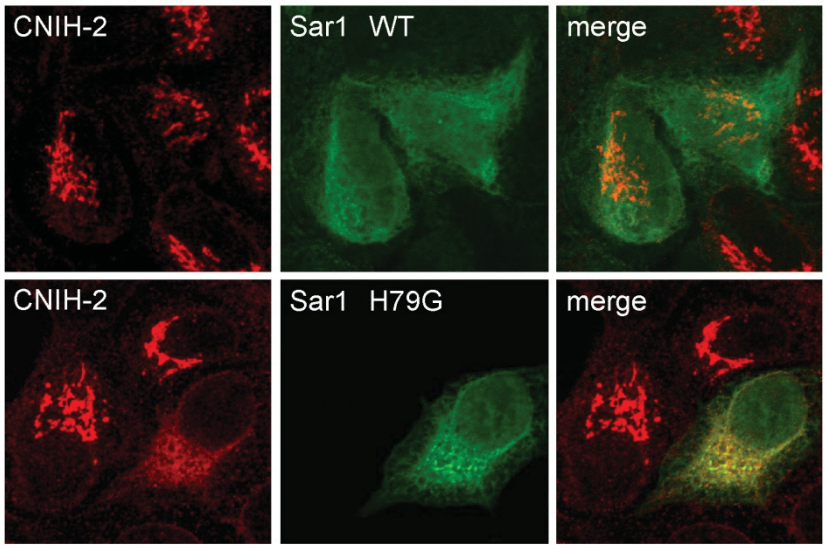

Fig 3-2. CNIH-2 is retained in the ER upon coexpression of dominant negative Sar1.
Representative confocal images of OK cells stably transfected with CNIH-2. In contrast to cells expressing Sar1 WT (upper panel), cells expressing mutant Sar1 H79G showed ER retention of CNIH-2 (lower panel). Modified from (Harmel, Cokic et al. 2012)

To find out whether also the increase in surface expression of AMPARs by CNIH-2 was dependent on COPII-mediated ER export, the above experiments were repeated with an extracellular epitope tagged GluA1 subunit, applying the surface epitope tagging assay (Fig. 3-3). A hemagglutinin (HA)-tag was inserted into the extracellular N-terminus of GluA1o, which enables to detect selectively the surface population of GluA1o in a detergent-free setup by an anti-HA antibody. HeLa cells were cotransfected with $GluA1_o$, CNIH-2, and either Sar1 wildtype or the mutant Sar1 construct, and $GluA1_o$ surface expression levels were quantified. For reasons of cell toxicity caused by general inhibition of ER export by dominant-negative Sar1, data had to be obtained already at 16 hours post-transfection. Co-expression of CNIH-2 elevated surface $GluA1_o$ expression by a factor of 1.7 ± 0.1 ($n = 12$; $p < 0.001$) in the presence of Sar1 WT. This increase was prevented in cells co-expressing dominant-negative Sar1 (1.0 ± 0.04; $n = 12$; $p = 0.732$).

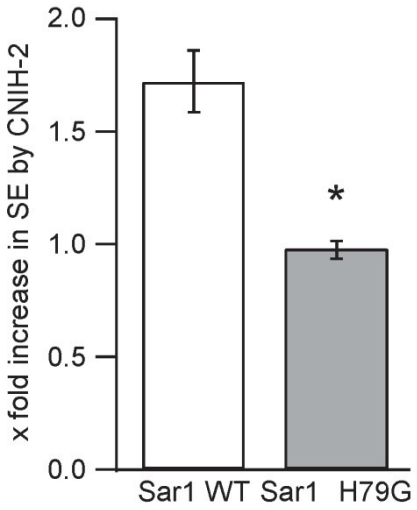

Fig 3-3. The AMPAR surface expression depends on COP-II facilitated CNIH-2 ER export.
Bar diagram depicts quantification of $GluA1_o$ surface expression levels in the presence of CNIH-2 and Sar1 WT (white bar) or $Sar1_{H79G}$ mutant (grey bar). Data show mean increases in surface expression levels by CNIH-2 ± SEM normalized to $GluA1_o$ + Sar1 WT or $GluA1_o$ + $Sar1_{H79G}$ without CNIH-2, respectively. Asterisk denotes a significant increase in surface expression of $GluA1_o$ by co-expression of CNIH-2 ($p < 0.001$, unpaired student´s t-test). Modified from (Harmel, Cokic et al. 2012)

Previously, it had been shown that CNIH-2 modulates AMPAR kinetics in heterologous expression systems and therefore must be part of heterologously assembled AMPAR complex on the cell surface. Here, we investigated whether CNIH-2 is integrated into AMPAR surface receptors also in neurons and may hence fulfill an essential criterion for an auxiliary subunit.

Postmitotic neurons are difficult to transfect. Therefore, primary hippocampal neurons were virally transduced by lentiviral gene transfer. Currents evoked by fast application of 10 mM glutamate were recorded from somatic outside-out patches. Currents from neurons overexpressing CNIH-2 displayed a significantly slower time course of desensitization (τ_{desens} = 11.1 ± 1.9 ms; $n = 8$; $p < 0.01$) than those received

from GFP-expressing sham-treated neurons used as control (τ_{desens} = 7.5 ± 3.4 ms; n = 19).

In summary, the obtained results show that CNIH-2 acts as an ER-cargo exporter of AMPARs. Furthermore, CNIH-2 modifies the electrophysiological properties of AMPARs expressed on the cell surface of dissociated hippocampal neurons.

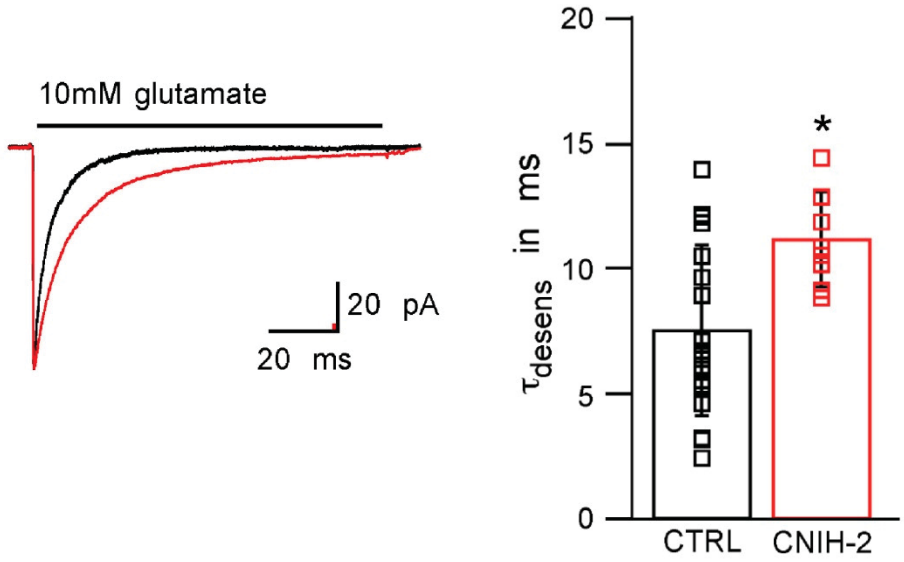

Fig. 3-4. CNIH-2 slows desensitization kinetics in hippocampal neurons.
Representative current traces recorded in somatic outside-out patches excised from dissociated hippocampal neurons (DIV 16-21) overexpressing either GFP (control) or CNIH-2 upon 100 ms application of 10 mM glutamate (top). Quantification of desensitization kinetics (bottom). Asterisk marks a significant difference from control ($p < 0.01$, unpaired student´s t-test; n = 19 for control and n = 8 for CNIH-2). Modified from (Harmel, Cokic et al. 2012)

3.2 Expression profiles of CNIH-2 and AMPARs are distinct during brain development

Whereas research on the cornichon isoforms has so far focused on its general cargo export function and lately also on the electrophysiological relevance of CNIH-2/3 as novel AMPAR complex constituents, the spatiotemporal expression profiles of CNIH-2/3 had remained unknown.

Immunohistochemical stainings had revealed that both CNIH-2 and CNIH-3 are rather ubiquitously expressed in various brain areas and cell types of the adult rat CNS (Schwenk, 2009). Yet, the antibody used in the mentioned study did not distinguish between the two CNIH homologues. Here, we intended to characterize the distribution of both isoforms in the developing brain and have employed a method that distinguished between the two homologues.

An in-situ hybridization study was performed on brain tissue sections to visualize CNIH-2 and CNIH-3 mRNAs at various developmental stages. Five time points in rat brain development were chosen: E18, P2, P10, P21, and adult (>P42).

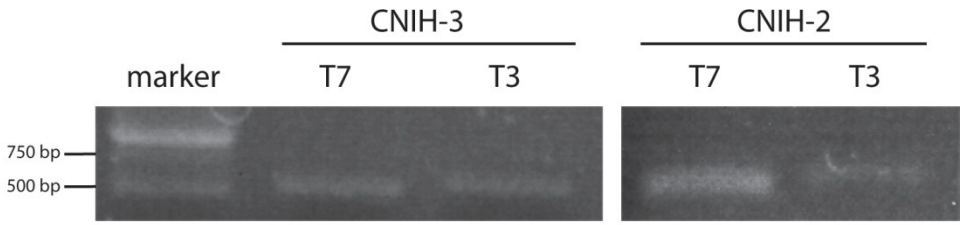

Fig 3-5: Detection of DIG-labeled CNIH-2 and CNIH-3 riboprobes.
CNIH-2 and CNIH-3 antisense (T7) and sense (T3) cRNAs were electrophoresed on an agarose gel and stained with ethidium bromide. Concentrations of full length CNIH-2 antisense (500 bp) and sense (510 bp) and CNIH-3 antisense (510 bp) and sense (530 bp) were estimated by comparison with the 500 bp marker band of known concentration: 0.1 µg/µl (CNIH-3; T7 and T3); 0.2 µg/µl (CNIH-2; T7) and 0.05 µg/µl (CNIH-2; T3).

First, full-length DIG-labeled CNIH-2 and CNIH-3 cRNAs were synthesized (Fig. 3-5). To determine cRNA concentrations, 5 µl of cRNA samples were loaded on a gel stained with ethidium bromide and signal intensities were compared with a 500 bp marker band that corresponds to 0.5 ng RNA. DIG-labeling of the riboprobes was of comparable efficiency as shown in Fig. 3-6.The specificity of the riboprobes for the respective target isoform of cornichon was ascertained by in-situ hybridization of HeLa cells previously transfected with CNIH-1 to 4 cDNAs. Antisense (T7) riboprobes recognized only respective target mRNA expressing cells. Control (T3, sense) riboprobes did not hybridize with any of the CNIH gene products (Fig. 3-7).

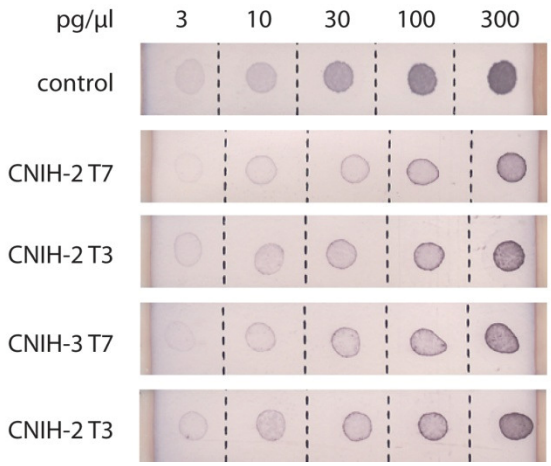

Fig. 3-6. DIG-labeling efficiencies of CNIH-2 and CNIH-3 riboprobes.
Testing efficiency of the labeling reaction of cRNAs using a dot blot. Serial dilutions of probes were spotted on test strips and after color reaction compared with signal intensities of the labeled control strip.

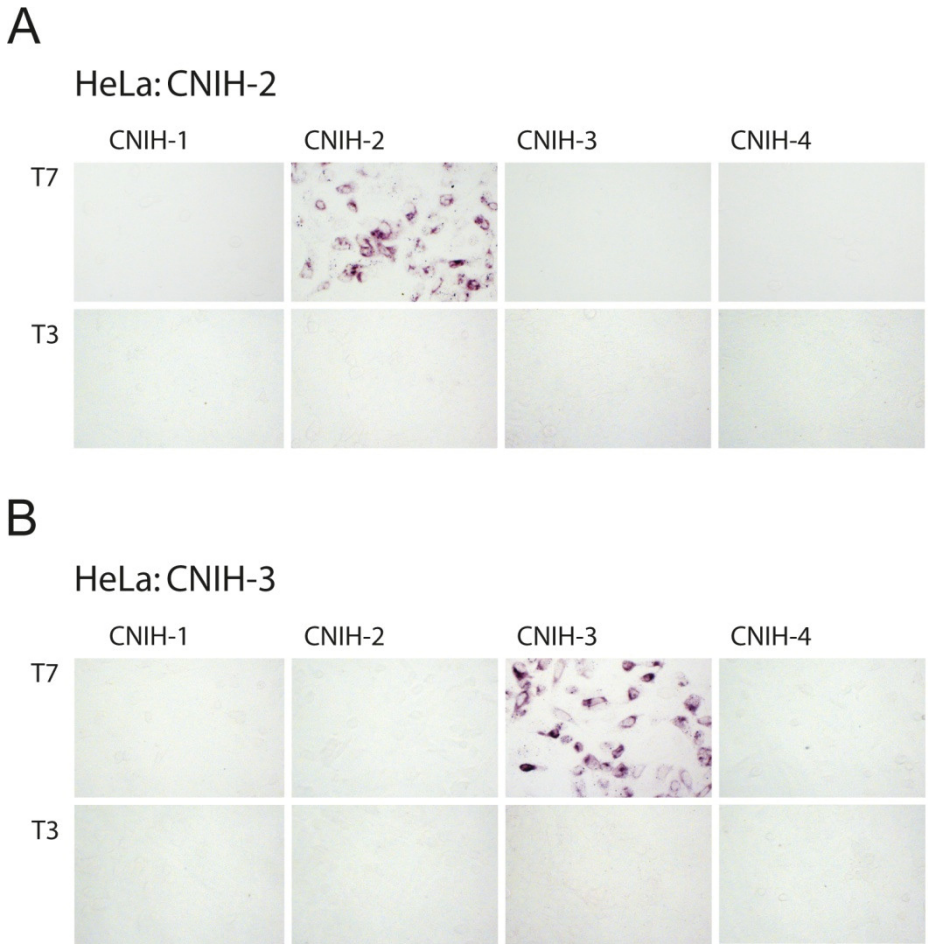

Fig. 3-7. Riboprobes distinguish between CNIH homologues.
CNIH-2 and CNIH-3 antisense (T7) and sense (T3) riboprobes were incubated with HeLa cells, expressing CNIH-1-4 homologues, respectively. T7 CNIH-2 and CNIH-3 cRNAs detected only target CNIH mRNAs. Modified from (Mauric, Molders et al. 2013)

In-situ hybridization of tissue sections in sagittal orientation revealed the presence of CNIH-2 and CNIH-3 mRNAs in the hippocampal formation and the neocortex. In contrast to CNIH-3, CNIH-2 was also expressed in the cerebellum. In order to compare signal intensities, all tissue sections were processed in parallel.

For CNIH-2 (Fig. 3-8), the strongest mRNA expression was detected at the two postnatal time points P2 and P10. Within the three investigated areas (hippocampus, neocortex, cerebellum), the localization of CNIH-2 positive cells was most stable in the hippocampal formation over development. From E18 onwards, CNIH-2 mRNA was expressed in the pyramidal cell layer of the developing CA subfields. At P2, CNIH-2 mRNA was also detectable in the dentate gyrus. At P21, CNIH-2 mRNA expression declined evenly in the entire hippocampal formation, but was still stronger than in the neocortex or cerebellum.

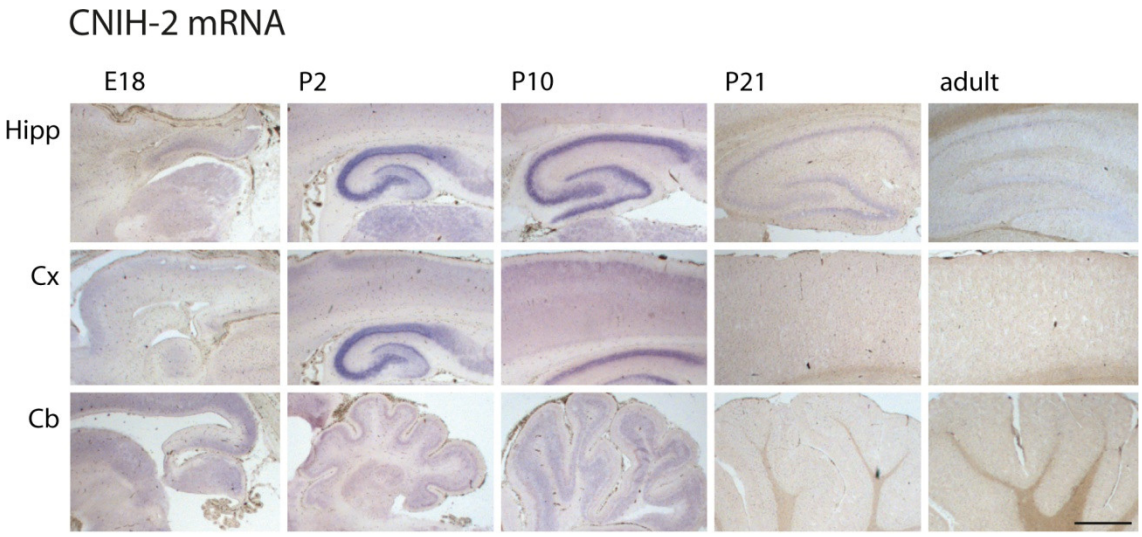

Fig. 3-8. Spatiotemporal expression profile of CNIH-2 mRNA in the developing rat brain. Representative images of CNIH-2 mRNA distribution in sagittal cryosections at indicated time points, detected by non-radioactive in-situ hybridization (n = 4). Panel represents one experimental run. CNIH-2 mRNA expression peaks in early postnatal stages in hippocampus (Hipp), neocortex (Cx) and cerebellum (Cb). All signal was absent in tissue, hybridized with sense probe. Anterior end is oriented to the left, scale bar: 500 µm. Modified from (Mauric, Molders et al. 2013)

Regional changes in CNIH-2 mRNA expression were observed in the developing neocortex (Fig 3-9): the prenatal cortical plate stained evenly positive for CNIH-2 mRNA, but at P2 the outermost layer of the cortical plate showed the strongest CNIH-2 mRNA expression that faded ventrally.

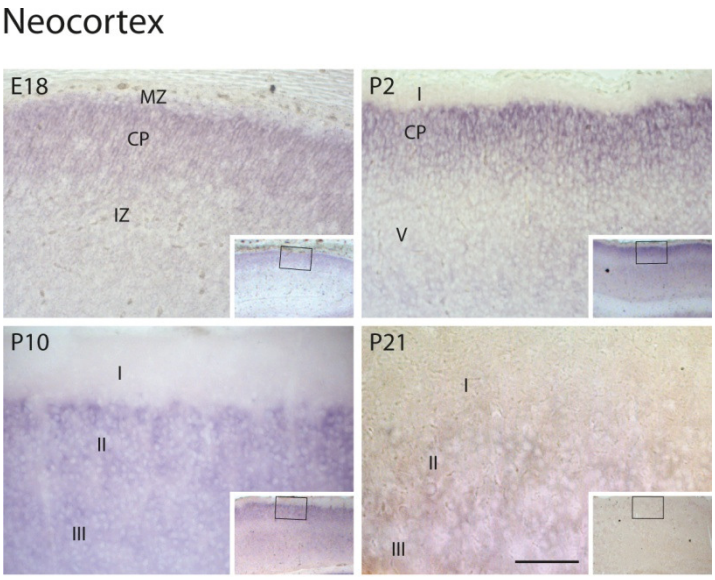

Fig. 3-9. CNIH-2 mRNA redistribution in the neocortex. Representative images of CNIH-2 mRNA expression in the neocortex, detected by non-radioactive in-situ hybridization. Higher magnification of insets revealed a distinct signal within the cortical plate (CP) at P2, which evenly redistributes with ongoing maturation. No signal was detected in sections hybridized with sense probes. MZ = molecular zone; I-V = neocortical layers; IZ = intermediate zone. Scale bar: 100µm. Modified from (Mauric, Molders et al. 2013).

This regional enrichment in CNIH-2 mRNA expression was lost three weeks after birth and CNIH-2 mRNA was then uniformly present throughout the neocortical cell layers.

The prenatal cerebellum displayed an abundant CNIH-2 mRNA distribution throughout the tissue underneath the external granule cell layer (EGL; Fig 3-10). Besides continuous CNIH-2 mRNA expression in the Purkinje cell layer, visible from P2 onwards, a temporary hybridization signal appeared in the internal granule cell layer (IGL) during the postembryonic process of cerebellar foliation. With the loss of the mitotic EGL three weeks after birth, CNIH-2 mRNA expression was confined to Purkinje cells.

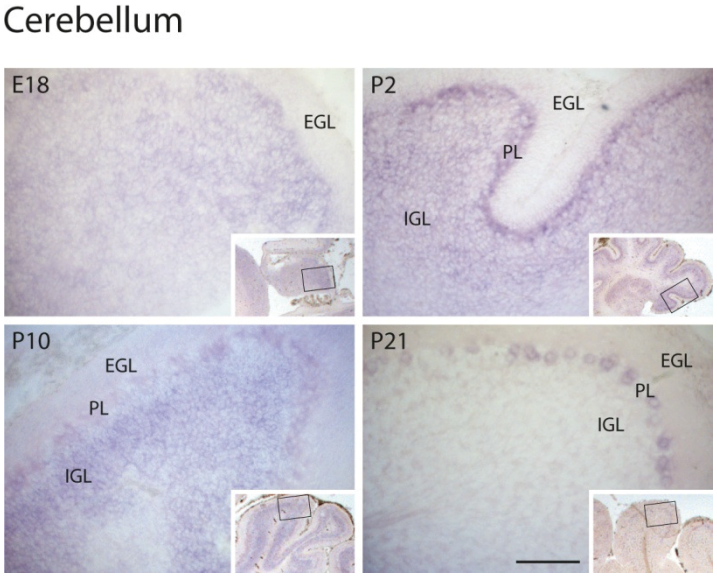

Fig. 3-10. CNIH-2 mRNA redistribution in the developing cerebellum. Representative images of CNIH-2 mRNA expression in the cerebellum, detected by non-radioactive in-situ hybridization. Higher magnification of insets revealed a temporary hybridization signal in the internal granule cell layer (IGL) beside constant CNIH-2 mRNA expression within the Purkinje cell layer (PL). Signal was absent in sections, hybridized with sense probe. MZ = molecular zone; EGL = external granule cell layer. Scale bar: 100µm. Modified from (Mauric, Molders et al. 2013).

Low levels of CNIH-3 mRNA (Fig 3-11) were present in the subiculum of the hippocampal formation at E18 and remained consistently expressed there until adulthood. Granule cells of the hippocampus started to express CNIH-3 mRNA from P10 onwards, a time point at which CNIH-2 mRNA was already highly expressed within this cell type. Further CNIH-3 mRNA expression was observed in the prenatal cortical plate, peaked within the first postnatal week and was still detectable at P21. Interestingly, the neocortical layer V, in which CNIH-3 positive cells were present, was located underneath the layer of the strikingly high expressing CNIH-2 mRNA cells. Thus, CNIH-3 mRNA levels showed a different distributional pattern and the transcript was present in less cellular subtypes compared to CNIH-2.

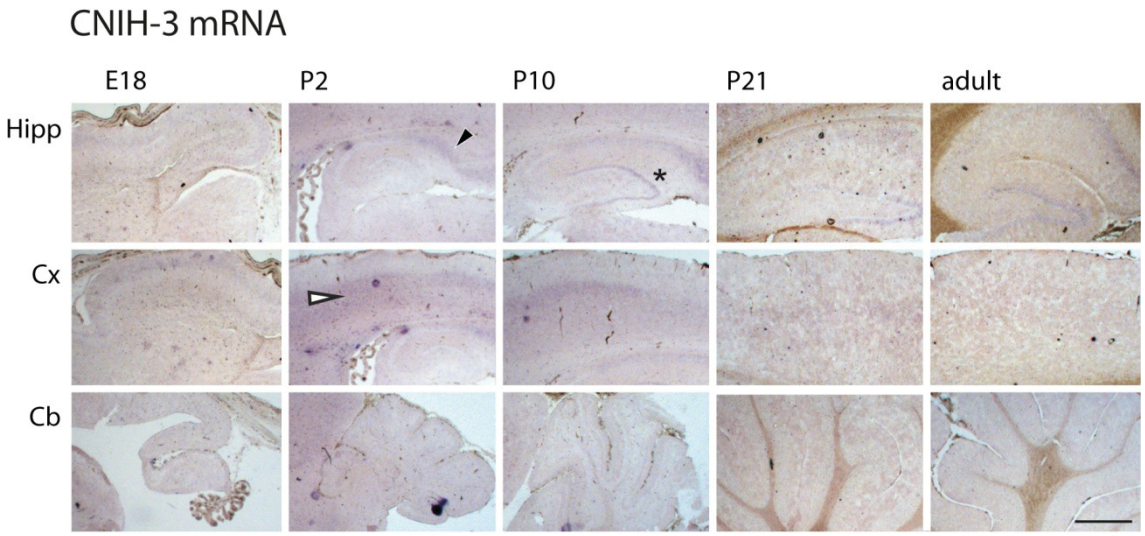

Fig. 3-11. Spatiotemporal expression profile of CNIH-3 mRNA in the developing rat brain. Representative image of CNIH-3 mRNA distribution in sagittal cryosections at indicated time points detected by non-radioactive in-situ hybridization (n = 2). Panel represents one experimental run. CNIH-3 mRNA expression is restricted to hippocampal granule cells (asterisk), the subiculum (black arrow) and the cortical plate (white arrow). All signal was absent in sections, hybridized with sense probe. Anterior end is oriented to the left, scale bar: 500 µm. Modified from (Mauric, Molders et al. 2013).

Next we tested whether the observed changes in CNIH-2 and CNIH-3 mRNA expression profiles during ontogeny are reflected at protein levels.

Immunohistochemical stainings were conducted in tissue sections using an antibody that recognizes both CNIH-2 and CNIH-3 isoforms (Hoshino, Uchida et al. 2007; Schwenk, Harmel et al. 2009). Protein expression levels were compared between P2 and P21 due to the fact that the steep decrease in CNIH-2 mRNA expression was obvious within this time interval and that detectable levels of the transcripts were present at both time points. The same exposure time was applied for stained sections from P2 and P21 individuals to be able to compare the CNIH-2/3 immunosignal. The CNIH-2/3 protein was abundantly expressed within the cortical plate and also in the pyramidal cells of the hippocampal CA1 region at 2 days after birth.

CNIH-2/3 were still expressed in the respective areas of P21 individuals although to much lesser extent (Fig. 3-12).

In the cerebellum, only the Purkinje cell layer contained CNIH-2/3 protein at P2 and P21, with no difference in intensity between these two time points.

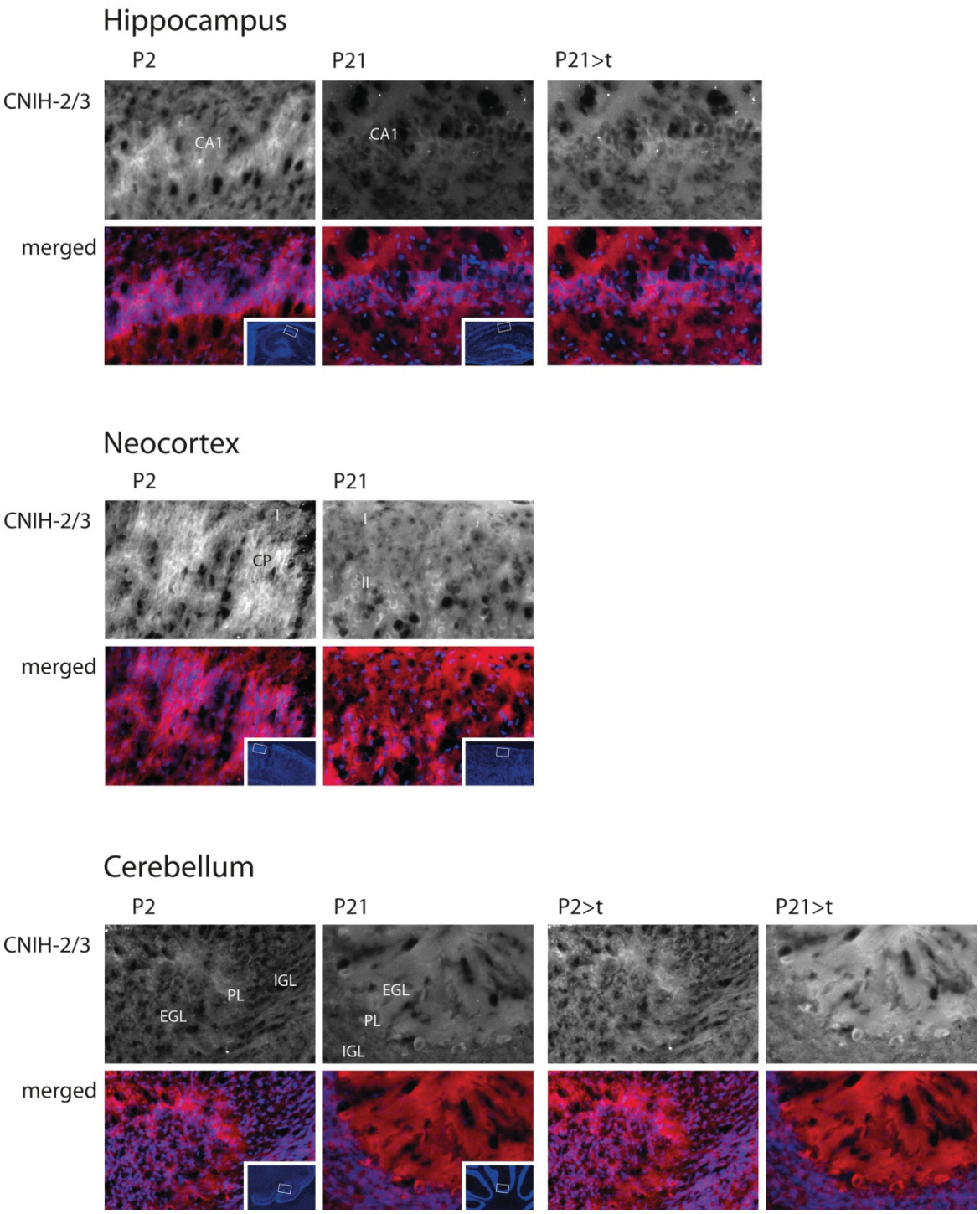

Fig. 3-12. CNIH-2/3 protein expression in the developing rat brain.

Representative immunofluorescence images of CNIH-2/3 protein expression in sagittal brain sections at P2 and P21. Panels represent immunosignal (CNIH-2/3) and the merge of immunosignal and DAPI staining (merged) in the hippocampus (upper panel), neocortex (middle panel), and the cerebellum (lower panel). Images were obtained with equal exposure time, except for ">t" indicating longer exposure time. Depicted are higher magnification views of boxed insets. Immunostaining revealed higher expression levels of CNIH-2/3 protein in pyramidal cells of the CA1, region (hippocampus) and in the cortical plate (CP; Neocortex) at P2 than at P21. Presence of CNIH-2/3 protein was observed in Purkinje cell layer (PL) at both time points with no increase in intensity and in radial glial fibers at P21.

Furthermore, the relationship of protein expression levels between the four AMPAR subunits GluA1 – 4 and the AMPAR complex constituents TARP-2/3, TARP-8 and CNIH-2/3 was studied in whole brain lysates during development.

GluA1 – 4 and the TARP proteins were present at E18, their expression increased continuously during postnatal time points and was then slightly decreased in adulthood. CNIH-2/3 protein behaved in an opposite manner; it was expressed at highest levels during the perinatal period and their expression declined with brain maturation (Fig. 3-13).

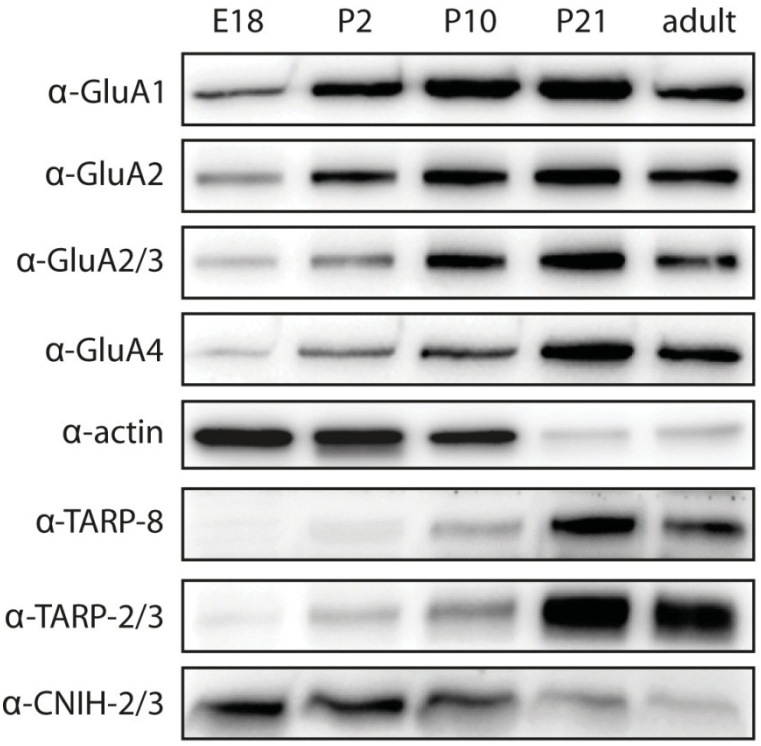

Fig. 3-13. Developmental protein expression patterns of the AMPAR constituents.
Representative Western blots of whole brain lysates isolated at indicated time points show reciprocal expression pattern of GluAs and TARPs on one side and CNIH-2/3 and actin on the other side. Modified from (Mauric, Molders et al. 2013).

Based on the fact, that the expression of commonly used loading controls such as β-actin and β-tubulin is also developmentally regulated (Bond & Farmer, 1983), protein expression of CNIH-2/3 was directly related to the one of GluAs at each time point (Fig. 3-14). Protein expression was detected by Western blot and quantified by densitometric analysis. The CNIH-2/3 to GluAx ratio decreased to an average of 10.9 ± 4.8 % (n = 4) in adult stage.

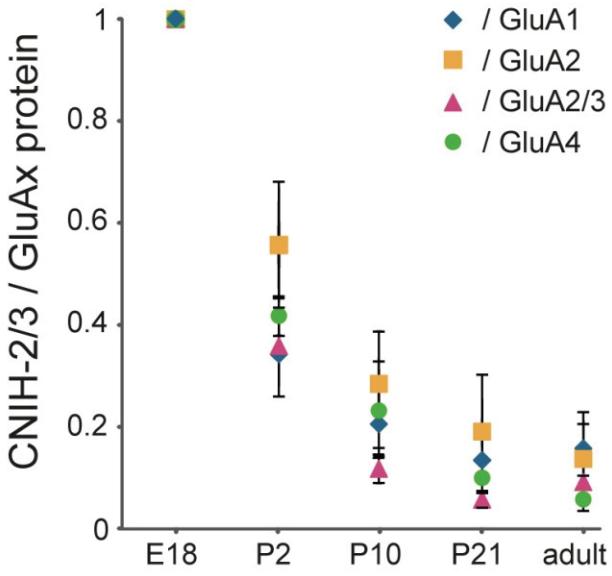

Fig. 3-14. Protein ratio of CNIH-2/3 and AMPAR decreases over development. Densitometric quantification of western blot results (n = 4). Depicted are CNIH-2/3 to GluAx ratios as indicated. Modified from (Mauric, Molders et al. 2013)

3.3 Stoichiometry of CNIH-2 and GluAs does not change during brain development

The above presented results (cf. 3.2) show that the GluAs and their interactors CNIH-2/3 exhibit opposite expression profiles. Whereas the expression of all four GluA subunits and TARPs increased in a similar manner during CNS maturation, the expression of CNIH-2/3 decreased. We therefore asked whether the stoichiometry, by which CNIH-2/3 assemble with GluAs, varied during the process of CNS maturation.
We chose to investigate AMPAR-CNIH-2/3 composition at the time point E18, when neural networks are just about to be formed and the role of AMPARs in this process is not fully understood yet. We compared AMPAR-CNIH-2/3 composition at E18 with the one at adult stage, where AMPARs function predominantly in basal glutamatergic transmission. Furthermore, these two time points were selected since the difference in protein expression was largest between these developmental stages.

We immunopurified all AMPARs using the following mixture of antibodies: 40% of anti-GluA2, 30% of anti-GluA1, 25% of anti-GluA2/3 and 5% of anti-GluA4 antibodies. This antibody ratio was adjusted to the relative GluA abundances in whole brain lysates as determined in Schwenk et al. (Schwenk, Harmel et al. 2012).
Immunopurification resulted in successful depletion of GluAs (Fig. 3-15) with efficiencies of 93 ± 0.04% and 96 ± 0.001% (GluA1), 89 ± 0.02% and 94 ± 0.02%; (GluA2/3) and 88 ± 0.04% and 92 ± 0.05% (GluA4) for E18 and adult, respectively. Only

depletion of GluA2 yielded a lower efficiency of 70 ± 0.02% at E18, when compared to the adult stage (96 ± 0.001%).

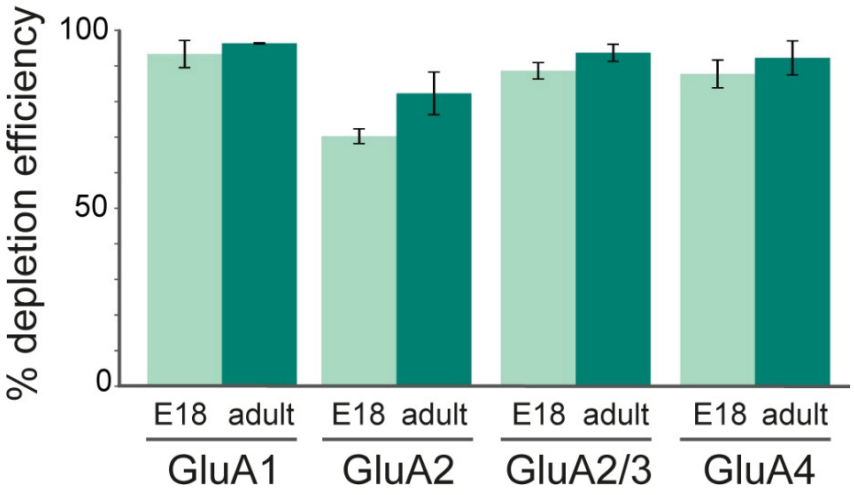

Fig. 3-15. Efficiency of GluA depletion from solubilized whole brain membranes.
Bar diagram summarizes mean efficiencies of depletion at indicated time points calculated from densitometric signal intensities as follows: 1-(unbound/load): GluA1 93 ± 0.04% and 96 ± 0.001%; GluA2 70 ± 0.02% and 82 ± 0.06%; GluA2/3 89 ± 0.02% and 94 ± 0.02%; GluA4 88 ± 0.04% and 92 ± 0.05%, for E18 and adult respectively. Modified from (Mauric, Molders et al. 2013).

Whole brain lysates (load) as well as the supernatant fraction after immunopurification containing unbound protein (unbound) and the eluate (IP; 10x concentrated) of E18 and adult material, were separated by SDS-PAGE and subjected to Western blot analysis (Fig. 3-15). Protein levels were quantified densitometrically.

Densitometrical data of the four GluAs obtained from one immunopurification experiment were averaged for respective time points and fractions. Corresponding CNIH-2/3 data were likewise averaged. E18/adult ratios of loaded and immunoprecipitated GluAs and CNIH-2/3 were calculated. Data from three independent experiments were combined.

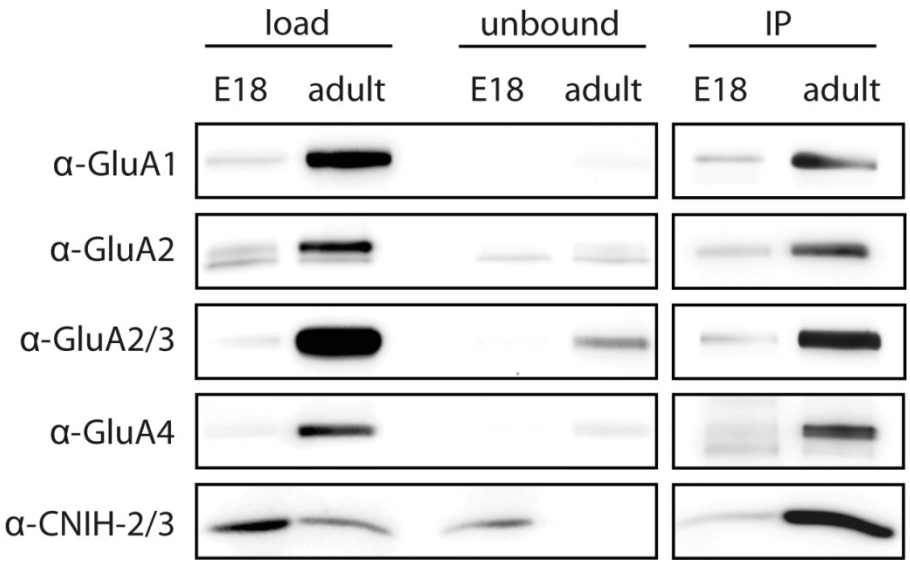

Fig. 3-16. Representative blots of immunoprecipitated GluAs and co-precipitated CNIH-2/3. Representative Western blots of affinity-purified GluA1-4 subunits and co-purified CNIH-2/3 proteins. Horizontal lanes probed with indicated antibodies were taken from the same blot membranes. Boxes mark different exposure times. Load = lysate; unbound = supernatant after anti-GluA1-4 affinity purification; IP = immunoprecipitated eluate. Modified from (Mauric, Molders et al. 2013).

Comparison of the E18/adult ratios of GluAs and CNIH-2/3 load fractions reflected the differences in developmental expression pattern as previously shown in Fig. 3-13. For the GluAs, the expression level increases with maturation (Fig. 3-13) and only 26 ± 0.12% of the amount present in adult stage were expressed in embryonic stage (Fig. 3-17). On the other hand, the embryonic amount of CNIH-2/3 exceeded the amount detected in adult stage by a factor of 2.4 ± 0.72.

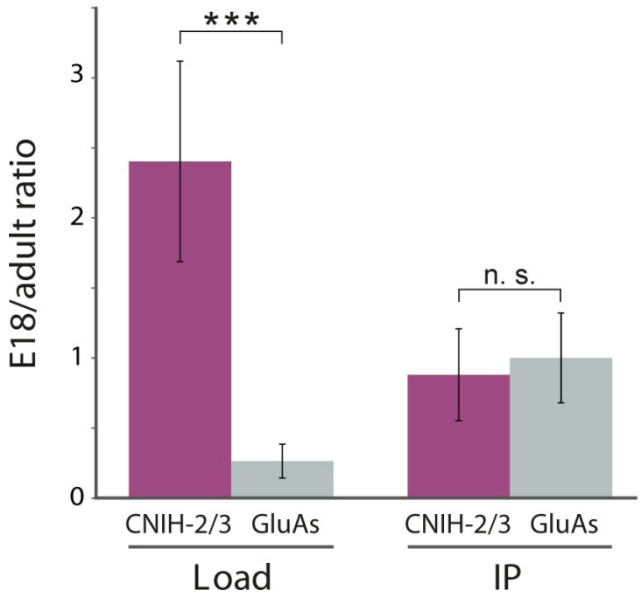

Fig. 3-17. AMPAR-free CNIH-2/3 protein levels declines during development.
Quantification of Western blots obtained after immunopurification (n = 3) shows densitometrically calculated E18/adult ratios for CNIH-2/3 and all GluAs in load and IP eluate (load = lysate; IP = immunoprecipitated eluate). Asterisks mark significant differences of E18/adult ratios in loads, $p < 0.001$). Note that the relative amount of co-precipitated, thus AMPAR-bound CNIH-2/3 does not change from embryonic E18 to adult stage (CNIH-2/3 IP: 0.87 ± 0.32; not significant (n.s.) from GluA1-4 IP 1 ± 0.31, p = 0.61). Modified from (Mauric, Molders et al. 2013).

Despite this obvious discrepancy between CNIH-2/3 and the GluAs in developmental expression, the ratio of this complex did not significantly change from E18 to adult stage (Fig. 3-17). The relative amounts of co-purified CNIH-2/3 (0.87 ± 0.32) were similar when normalized to those of immunopurified GluAs (1 ± 0.31).
The finding that there is a large fraction of AMPAR-free CNIH-2/3 at E18 raises the intriguing possibility of another particular function for cornichons at early developmental stages.

3.4 HB-EGF as a putative cargo substrate of CNIH-2?

The previous results indicate that the opposite expression profiles of CNIH-2/3 and GluAs do not lead to developmentally variant stoichiometries. We therefore speculated that the apparently AMPAR-free CNIH-2/3 at embryonic stages might exert another function than being an AMPAR auxiliary subunit.
Of the identified growth factors of the EGF superfamily that are trafficked by cornichon orthologs, rodent HB-EGF exhibits a strikingly similar mRNA expression pattern as rat

CNIH-2 (Kornblum, Zurcher et al. 1999). Moreover, it was shown that during chicken development the chicken CNIH-2 ortholog facilitates the secretion of HB-EGF. After being glycosylated in the Golgi apparatus, the transmembrane form of this growth factor is trafficked to the cell surface. Once it has arrived there, it can be cleaved by metalloproteinases giving rise to a soluble form and a remaining transmembrane part of HB-EGF (Toki, Nanba et al. 2005).

We wanted to investigate a putative functional interaction between CNIH-2 and HB-EGF by evaluating whether CNIH-2 co-expression leads to changes in the amount of surface HB-EGF. For this purpose, we applied the surface epitope tagging assay again.
It was first tested whether a commercially available antibody against the C-terminus of human HB-EGF recognized rat HB-EGF. A fusion protein of HB-EGF-GFP was overexpressed in HeLa cells and antibody specificity was controlled by colocalization of GFP expression and HB-EGF staining (C, Fig. 3-18). To exclude trafficking delays by GFP fusion, we conducted the surface epitope tagging assay with the untagged HB-EGF construct (D, Fig. 3-18).

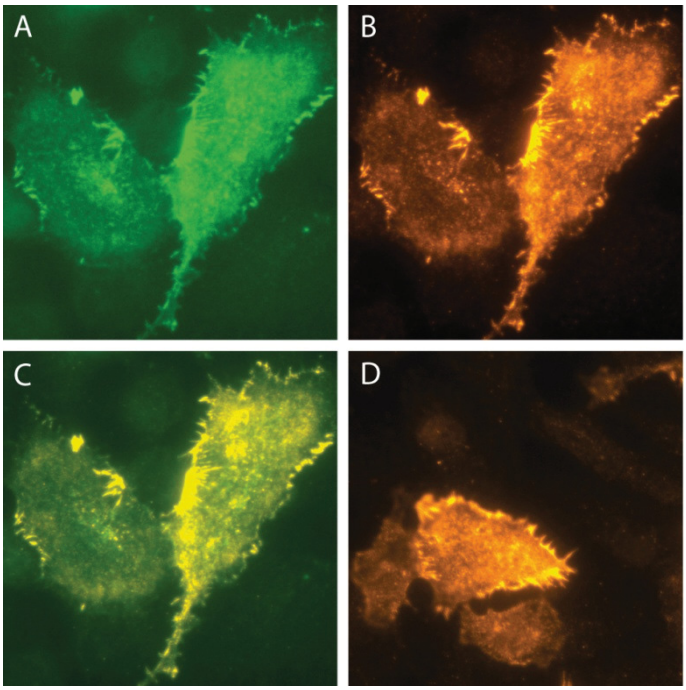

Fig. 3-18. α-HB-EGF recognizes the transmembrane precursor form of HB-EGF at the plasma membrane. Representative immunofluorescence images of exogenously expressed GFP-tagged (A, B, C) and untagged (D) rat HB-EGF in HeLa cells**.** GFP-signal (A) and α-HB-EGF immunostaining (B) of C-terminally GFP tagged rat HB-EGF show co-localization (merged image, C) at the plasma membrane. HeLa cells expressing the un-tagged rat HB-EGF construct exhibit the same immunopattern when stained with α-HB-EGF.

Surface expression of HB-EGF increased upon its overexpression (control, 0.36 ± 0.06, p = 0.96, n = 4) indicating that the surface population of rat HB-EGF could be further

elevated in HeLa cells, which are known to express this growth factor endogenously (Wang, Liu et al. 2007).

When compared to the control condition, HB-EGF surface expression increased upon co-expression with CNIH-1 (2.99 ± 1.34; p = 0.17, n = 7), CNIH-2 (1.13 ± 0.10, p = 1, n = 16), and CNIH-3 (1.63 ± 0.02, p = 0.99, n = 3). CNIH-4 co-expression on the other hand decreased HB-EGF surface population (0.7 ± 0.1; p = 1, n= 3). The mean values of experimental groups were highly spread and no significant difference compared to the control condition could be determined.

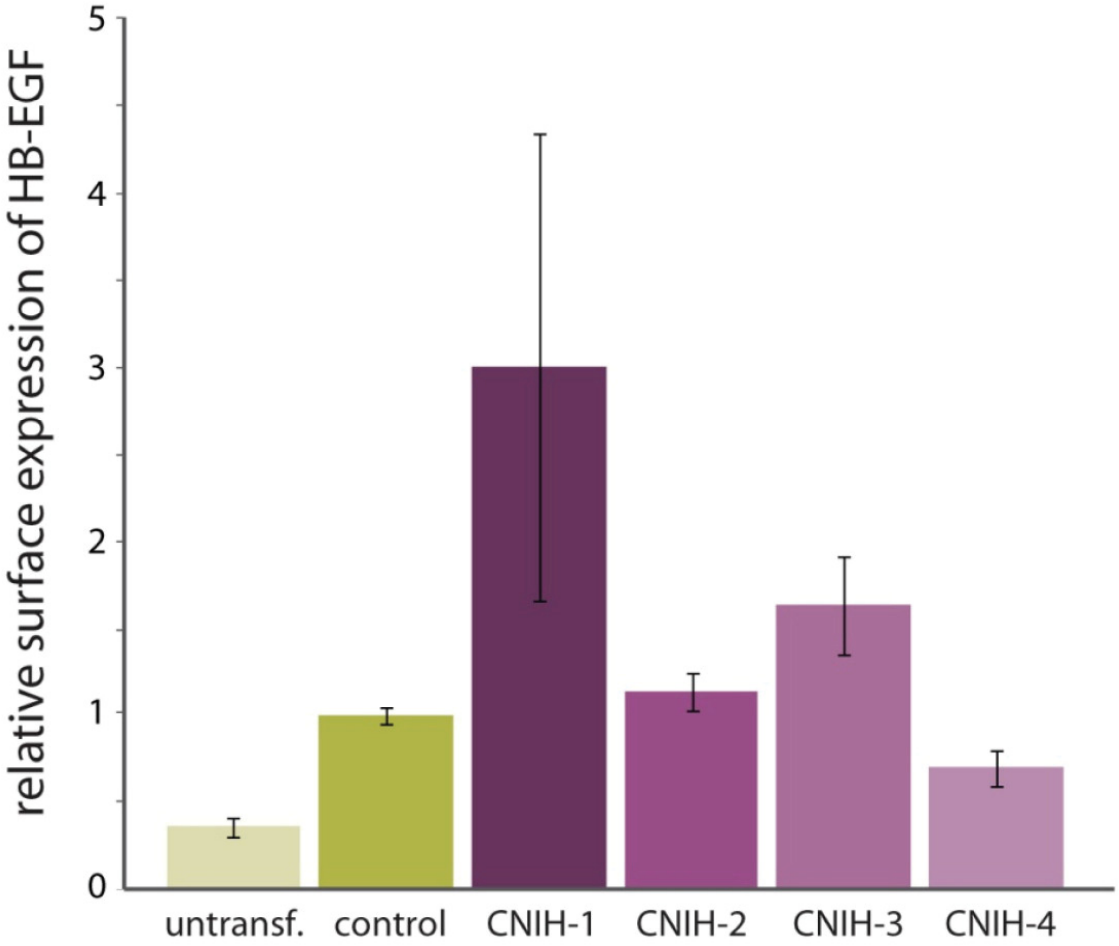

Fig. 3-19. Changes in surface expression of HB-EGF upon cornichon co-expression.
Quantification of HB-EGF surface expression levels by extracellular epitope tagging in the presence of cornichon homologues 1-4 (purple bars) and calmodulin (control, yellow bar). Data are mean increases in surface expression levels by cornichons ± SEM normalized to HB-EGF + calmodulin. One way ANOVA with Scheffé post-hoc test was applied to calculate significant differences.

To determine whether HeLa cells express cornichons endogenously, which may have precluded the anticipated changes in HB-EGF surface expression, we characterized the

expression of human cornichon orthologs in this cell line via the reverse transcriptase polychain reaction (RT-PCR) method (Fig 3-20).

A gradient RT-PCR was performed on a cDNA library generated from HeLa cells or with water as a control, using specific primers for human CNIH-1 to 4. PCR amplification (30 cycles) gave rise to single bands of expected size only in cDNA samples containing either CNIH-1 or CNIH-2 primers respectively. To verify the identity of the amplicons, they were subcloned into the pcDNA3.1. After sequencing of both products, alignment of the CNIH-1 bearing vector showed 100% sequence identity of the human reference sequence (pubmed NM_005776.2). In contrast, the CNIH-2 product was identified as a mutant rat CNIH-2 contamination, previously generated in the lab. Our results show that HeLa cells express endogenous CNIH-1, but not CNIH-2.

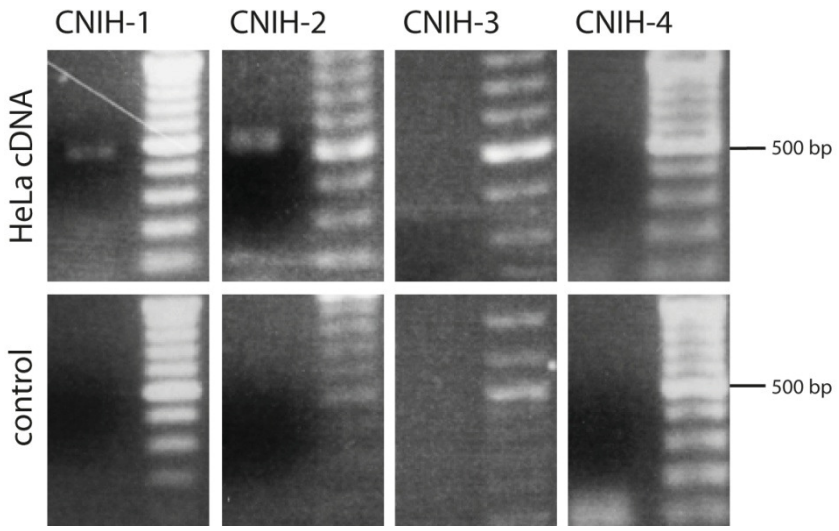

Abb. 3-20. Evaluation of endogenous cornichon isoform expression in HeLa cells.

Agarose gel electrophoresis of reverse-transcriptase PCR products obtained with primers for human CNIH-1 - 4 from HeLa cell cDNA (upper panel) or water (control, lower panel). Single images contain PCR product (left lane) and ladder (right lane). Amplicon size: CNIH-1: 490bp; CNIH-2: 510bp.

4. Discussion

4.1 AMPARs recruit an ER cargo exporter to the cell surface for signaling

Affinity purification of native AMPAR complexes from adult rat brain and subsequent mass spectrometric analyses have revealed a novel group of protein complex constituents, the cornichons (Schwenk, Harmel et al. 2009). In reconstitution assays using HeLa cells and Xenopus laevis oocytes, the number of AMPARs expressed at the plasma membrane increased upon co-expression of the two cornichon homologues CNIH-2 or CNIH-3. Further, the expression of cornichons altered AMPAR kinetics in oocytes.
A follow-up study by Shi and co-workers published about cornichons in this context was able to reproduce the observed effects of CNIH-2 on the AMPAR in HEK cells but failed to detect CNIH-2 at the cell surface in neurons (Shi, Suh et al. 2010). Also, when overexpressed in cerebellar granule cells cultured from heterozygous stargazer mice, CNIH-2 was able to increase the low levels of surface AMPARs in these neurons, but these additionally trafficked AMPARs did not display the peculiar kinetics of AMPARs associated with CNIH-2. The group therefore speculated, that CNIH-2 served a similar role for the AMPAR as the one described for its orthologs in trafficking growth factors (Powers and Barlowe 1998; Castro, Piscopo et al. 2007). The authors proposed that CNIH-2 indeed exported AMPARs from the ER, but without being associated with the AMPAR at the plasma membrane (Shi, Suh et al. 2010). Possible reasons for these different observations might have been differences in experimental protocols and reagents (Brockie and Maricq 2010).

In the present study, we showed that CNIH-2 co-localized with Golgi markers as well as with the small GTPase Sar1, a component of the COPII export machinery (Lee and Miller 2007). In the presence of Sar1 H79G, a dominant negative mutant of Sar1 unable to hydrolyze GTP and hence blocking ER-to-Golgi export (Aridor, Bannykh et al. 1995), we found CNIH-2 redistributed into the ER. It finally behaved like any other Golgi-resident protein known to cycle between the ER and the Golgi apparatus with an increased dwell time in the Golgi (Storrie, White et al. 1998; Ward, Polishchuk et al. 2001).
Intriguingly, the observed increase in AMPAR surface levels in the presence of Sar1 and CNIH-2 was abolished upon co-expression of CNIH-2 and the Sar1 mutant. These results

strongly suggest that the CNIH-2 mediated increase in the AMPAR surface population relies on COPII-dependent ER export.
In contrast to the study of Shi et al., presence of CNIH-2 at the plasma membrane was determined by electrophysiological recordings showing that AMPARs were modulated by CNIH-2 overexpression. Our results are in good agreement with data from other groups, demonstrating the presence of CNIH-2 in postsynaptic hippocampal AMPARs by the electrophysiological phenomenon of resensitization (Kato, Gill et al. 2010).
Taken together, our results show that CNIH-2 initially acts as an ER-cargo exporter of the AMPAR and is then converted into an auxiliary subunit of the receptor.

4.2 Expression of CNIH-2/3 decreases in development contrasting the expression profile of AMPARs

Up to this study, expression data of the newly identified AMPAR auxiliary subunits CNIH-2/3 were so far only available at protein levels and for adult animals (Schwenk, Harmel et al. 2009).
Hence, the expression pattern of CNIH-2 and CNIH-3 was characterized at time points spanning neuronal development from embryonic day E18 to adulthood. CNIH-2/3 were expressed at all time points investigated. We found CNIH-2 and CNIH-3 expression to peak in early ontogenesis, with local changes in their expression pattern during perinatal stages.

In situ hybridization was chosen as the experimental set-up in order to examine the distinct expression pattern of CNIH-2 and CNIH-3. Expression of CNIH-2 mRNA was sufficient to explain the stainings achieved by the antibody in the previous expression analysis recognizing both CNIH-2 and CNIH-3 isoforms (Schwenk, Harmel et al. 2009). The in situ data revealed that unlike CNIH-2 mRNA, which was expressed in all areas investigated, CNIH-3 mRNA expression was rather limited to the hippocampus and cerebellum.

At embryonic stage, CNIH-2 mRNA was evenly expressed within the primordial layers of investigated brain areas. Out of these regions, CNIH-2 mRNA was evenly expressed throughout the CP within the neocortex. In this brain area, newly born neurons migrate from the ventricular zone (VZ) towards the pial surface and settle on top of the just previously born neurons (reviewed in (Hatten 1999). During this stage of neocortical lamination, most migrating cells are neurons (Rao 2005). In contrast to the CP neurons, cells of the VZ (neurogenic niche located underneath the IZ) as well as cells of the MZ

appeared to be devoid of CNIH-2 mRNA. These two layers are known to be established in early neuronal development, before the first cohort of migrating cortical plate neurons emerge (reviewed in (Kriegstein and Noctor 2004). The ventricular layer has been described to contain primarily somata of radial glial cells that build the scaffold for neurons along which they move (Bentivoglio and Mazzarello 1999). The MZ displays specialized neurons, the so called Cajal Retzius cells. Thus, CNIH-2 mRNA is mainly expressed by migrating, neocortical neurons.
Similar to the neocortex, the cerebellum also exhibited cells within the primordial areas, that evenly expressed CNIH-2 mRNA, while the above situated cells of the EGL were devoid of CNIH-2 mRNA. The EGL contains proliferating, premigratory cells. Upon the last cell cycle, EGL cells migrate inwardly to reach the layer that later builds the EGL (Altman 1997).
Taken together, CNIH-2 mRNA is expressed by postmitotic, migrating neurons at this stage, without differences in expression intensity between earlier or later born neurons.

At perinatal stages, the distribution of the transcript changed, now showing stronger expression in particular cell layers.
Within the neocortex, CNIH-2 mRNA levels were highest in superficial levels of the CP underneath the MZ, which is the future neocortical layer I (Angevine and Sidman 1961). This gradient expression of CNIH-2 mRNA was reminiscent of the maturation pattern, described for the layering of the perinatal neocortex (reviewed in (Gupta, Tsai et al. 2002; Diaz and Gleeson 2009), . The layer with the highest CNIH-2 transcript expression corresponded to newly arrived neurons, which are in the process of detachment upon binding of Reelin, secreted from juxtaposed MZ Cajal Retzius cells (Pinto-Lord, Evrard et al. 1982).
Besides acting as a guidance cue and stop signal for migrating neurons (reviewed in (Tissir and Goffinet 2003), Reelin was also shown to act on AMPARs as secretion of Reelin leads to increased surface levels of AMPARs (Qiu, Zhao et al. 2006). It is noteworthy, that the GluA1 subunit has been shown to be expressed particularly in the superficial layers of the neocortex during the first postnatal week (Martin, Furuta et al. 1998). This may be explained by the involvement of AMPARs in terminal differentiation processes of settled neurons, such as dendritogenesis and synaptogenesis in newly settled neurons (reviewed in (Super and Uylings 2001; Hamad, Ma-Hogemeier et al. 2011).
The cerebellum also displayed temporal changes in CNIH-2 mRNA distribution. At first, the transcript was present in the IGL zone in the first two weeks after birth before being downregulated. This cell layer consists of neurons that have previously migrated from the EGL through the PL (Purkinje layer) into the IGL (Miale and Sidman 1961). The migration process peaks during the first two postnatal weeks (reviewed in (Goldowitz

and Hamre 1998). In contrast to the absence of AMPARs in the EGL (Ripellino, Neve et al. 1998), AMPARs were shown to be expressed in the IGL at this time. The authors of the latter study speculated that AMPARs were expressed on these cells in order to prepare for impending synaptogenesis (Smith, Wang et al. 2000).
Therefore, elevated CNIH-2 mRNA expression within these cell layers of different brain areas might reflect the need of the AMPAR for regulated export rates and gating kinetics.

Three weeks after birth, the overall CNIH-2 mRNA expression was downregulated to adult levels within the neocortex and the cerebellum. Loss of the distinct expression pattern of CNIH-2 coincided with the terminated migration process in the cerebellum (Altman 1997) and developmentally regulated transition of network activity. This transition is marked by the loss of synchronized patterns of activity in early development and emergence of decorrelated activity (Golshani, Goncalves et al. 2009) after neuronal migration in the neocortex. It seems therefore likely, that later in development, CNIH-2 may serve a role in modulating AMPAR expression in events of synaptic plasticity.

The protein expression profile of AMPAR pore-lining GluA subunits revealed an increase of all four subunits during development. Our results are in line with literature, describing functional AMPARs to be expressed as early as E15 in the hypothalamus, right at the beginning of neurogenesis within this region (van den Pol, Obrietan et al. 1995) and GluA1 protein to be detectable in whole brain lysates from E14/E15 onwards (Martin, Furuta et al. 1998). Furthermore, mRNA levels of GluAs were described to increase steadily during brain maturation with highest levels in the third postnatal week (Pellegrini-Giampietro, Bennett et al. 1991).
The expression profiles of the exclusive AMPAR auxiliary subunits TARP-2/3 and TARP-8 were detectable at E18 and increased with ongoing maturation. This is in good agreement with a report by Tomita et al. showing an increase in expression of these TARP isoforms from neonatal to adult stage (Tomita, Chen et al. 2003). The recently identified AMPAR constituent neuritin (Schwenk, Harmel et al. 2012) is expressed on mRNA level as early as E14/E15 (Putz, Harwell et al. 2005) and increases in expression have been described for the neocortex and hippocampus in postnatal development (Naeve, Ramakrishnan et al. 1997). Thus the expression profiles of AMPAR auxiliary subunits basically parallel the one of GluAs.
In sharp contrast, however, the expression profile of CNIH-2/3 was opposite, both at mRNA and protein level.

4.3 Most CNIH-2 is AMPAR-free in early ontogenesis

Comparison of the developmental expression profiles of CNIH-2/3 and the GluAs shows a reciprocal relation. Elevated expression of CNIH-2/3 in early development could be explained by (1) a variant stoichiometry of the CNIH-2/3 / AMPAR complex during this time or (2) by serving a function apart from being an AMPAR auxiliary subunit.

(1) We tested whether the amount of CNIH-2/3 being integrated into AMPAR complexes changed from E18 to adult stage.
The highly discrepant developmental expression profiles of GluAs and CNIH-2/3 were not paralleled in co-purification experiments depleting all AMPARs from solubilized brain membranes at embryonic versus adult stages. At E18, only a minor percentage of total CNIH-2/3 was associated with GluAs, while in adult stages almost all of the available CNIH-2/3 was integrated into the AMPAR complex. From this, it can be concluded that the role of CNIH-2/3 gains importance as an AMPAR auxiliary subunit in the course of brain maturation.
One possible explanation for the ontogenic recruitment of CNIH-2/3 into AMPAR complexes may be an extraordinarily high affinity of GluAs for the auxiliary subunit. Such view is supported by our finding that during phylogeny the ancient ER cargo exporter cornichon is caused to leave its ER-to-Golgi cycle by interaction with GluAs, which are then accompanied by CNIH-2/3 all the way to the cell surface.
Furthermore, RNA editing of a glutamine (Q) residue to arginine (R) at position 607 of the GluA2 subunit is developmentally regulated, with virtually all GluA2 at adult stage being edited (Sommer, Keinanen et al. 1990). As the edited GluA2 reaches the plasma membrane much slower than the unedited isoform (Greger, Khatri et al. 2002) and may therefore rely on CNIH-2/3 mediated ER export to be efficiently trafficked to the plasma membrane.

(2) The large pool of AMPAR-unbound CNIH-2/3 at E18 raised the question, whether CNIH-2/3 might serve another role. Various cornichon orthologs across species function as ER cargo exporters for growth factors of the EGF superfamily (Bokel, Dass et al. 2006; Castro, Piscopo et al. 2007; Hoshino, Uchida et al. 2007).
It has been reported, that proteins with similar expression pattern have a high probability to functionally interact (Bhardwaj and Lu 2005). Searching for putative cargo proteins of CNIH-2 other than AMPAR, we looked at the expression patterns of EGF-like growth factors published in the literature. Of the described expression patterns of EGF-

like growth factors (Anton, Ghashghaei et al. 2004), temporospatial distribution of HB-EGF matched the ones of CNIH-2 and CNIH-3 the most.

In situ hybridization detected HB-EGF mRNA in the neocortex at E14, with intense expression in the superficial neocortical layers, within the hippocampal formation and in the Purkinje cell layer in late embryonic to perinatal stages (Kornblum, Zurcher et al. 1999). These are in particular the cell layers and cell populations, where CNIH-2 mRNA was detected the strongest. Therefore, the ER export of rat HB-EGF with each of the four cornichon homologues was assayed in vitro by quantifying the levels of HB-EGF surface expression upon co-expression.

The balance between mature and immature protein levels of the growth factor TGF-alpha was shifted in the presence of CNIH-1 in HeLa cells. Co-expression of CNIH-1 leads to decreased levels of mature TGF-alpha but increased levels of the immature and intracellularly retained form, as a result of the regulatory function of CNIH-1 on TGF-alpha secretion (Castro, Piscopo et al. 2007).

Of the four homologues tested, CNIH-1 led to the highest increase in HB-EGF surface expression, but collected data were not significant due to large standard deviation. In contrast to CNIH-1, CNIH-2 had no detectable effect on the surface presentation of HB-EGF. RT-PCR confirmed endogenous presence of CNIH-1, in line with immunostainings on endogenous CNIH-1 in HeLa cells (Castro, Piscopo et al. 2007), and excluded the endogenous expression of other cornichon homologues. Therefore CNIH-1 appears to be more appropriate for a role in trafficking exogenously expressed HB-EGF but also of endogenous HB-EGF (Wang, Sloss et al. 2007) than CNIH-2.

To exclude that our results differ from the published observations on TGF-alpha trafficking by CNIH-1 because of disrupted plasma membrane, leading to HB-EGF antibody binding of the intracellular fraction and therefore mimicking high surface levels, another experimental set-up should be chosen.

.

5. Summary

The cornichon (CNIH) family of proteins is highly conserved among species. Orthologs serve as ER cargo exporters for precursors of growth factors of the EGF superfamily and other single pass transmembrane proteins. Recently, using a proteomic based approach, the mammalian cornichon homologues CNIH-2 and CNIH-3 have been identified as constituents of native glutamate receptors of the AMPA subtype (AMPARs) in rat brain. Heterologous reconstitution experiments have shown that CNIH-2/3 increase AMPAR levels at the plasma membrane and modulate the biophysical properties of the channel (Schwenk, Harmel et al. 2009).

This work aimed to elucidate the molecular mechanism underlying the increase in the surface population of AMPARs and to characterize the ontogenetic expression pattern of CNIH-2/3 in rat brain.

Using immunocytochemistry, the results show that CNIH-2 usually resides within the early secretory pathway. Functional studies demonstrate that CNIH-2 facilitates the delivery of AMPARs via COPII dependent ER export, thereby increasing the plasma membrane population of AMPARs. The interaction of CNIH-2 and AMPAR forces CNIH-2 to leave its ancestral localization and to accompany the AMPAR to the plasma membrane where it remains within the channel complex to alter the signaling properties of the AMPAR.

Developmental expression profiles of CNIH-2 and CNIH-3, assessed at mRNA level by non-radioactive in-situ hybridization and at protein level by immunoblot analysis, exhibit elevated expression in late embryogenesis and a decline in expression towards adult stage. Surprisingly, the pore-lining AMPAR GluA subunits as well as prototypical auxiliary subunits as the transmembrane AMPAR regulatory proteins (TARPs) show an expression pattern reciprocal to the one of CNIH-2/3. Co-immunoprecipitation analysis, however, reveals that CNIH-2/3 integrate into AMPAR complexes at similar ratios both at embryonic and adult stage of development. Thus, there is a large pool of AMPAR-free CNIH-2/3 in early development, which might serve other roles than being an AMPAR auxiliary subunit.

In summary, the present study shows that CNIH-2/3 operates both as an ER cargo exporter and, if AMPARs are present, as their auxiliary subunit. Given the reciprocal expression profiles of CNIH-2/3 and the pore-forming GluAs but their constant ratio of co-assembly during ontogenesis, the data strongly suggest that in early development, CNIH-2/3 fulfills functions in addition to being an AMPAR constituent, i.e. ER cargo export of growth factors.

6. Zusammenfassung

Verschiedene Orthologe der hochkonservierten Familie der Cornichon Proteine (CNIH) exportieren transmembranäre Vorläuferformen von Wachstumsfaktoren sowie bestimmte Typ-1 Transmembranproteine aus dem endoplasmatischem Retikulum (ER). In einer Proteomanalyse sind darüber hinaus die Säugetier-Homologe CNIH-2 und CNIH-3 als Bestandteile nativer Glutamatrezeptorkomplexe vom AMPA-Subtyp im zentralen Nervensystem (ZNS) der Ratte identifiziert worden (Schwenk et al, 2009). Experimente in heterologen Expressionssystemen haben gezeigt, dass die Koexpression von CNIH-2/3 die Anzahl der AMPA-Rezeptoren an der Zelloberfläche (Oberflächenexpression) erhöht und die elektrophysiologischen Eigenschaften des AMPA-Rezeptors moduliert.
Ziel der vorliegenden Arbeit war (1) die Identifizierung der molekularen Mechanismen, die der erhöhten Oberflächenexpression der AMPA-Rezeptoren bei Koexpression von CNIH-2/3 zugrunde liegen und (2) die Charakterisierung des ontogenetischen Expressionsprofils von CNIH-2/3 im ZNS der Ratte.

Mittels Immunzytochemie wurde CNIH-2 im frühen sekretorischen Transportweg, d. h. im ER und Golgi-Apparat nachgewiesen. Funktionelle Experimente konnten zeigen, dass CNIH-2 den Export von AMPA-Rezeptoren aus dem ER in einem COPII-abhängigen Mechanismus fördert und dadurch die Oberflächenexpression der Rezeptoren erhöht. Durch Interaktion mit dem AMPA-Rezeptor verlässt CNIH-2 seine ursprüngliche subzelluläre Lokalisation und gelangt zusammen mit den Rezeptoren zur Plasmamembran. Dort verbleibt es im Rezeptorkomplex und verändert dessen biophysikalische Eigenschaften.
Die ontogenetischen Expressionsprofile von CNIH-2 und CNIH-3 wurden auf Ebene der mRNA mittels nicht-radioaktiver in-situ Hybridisierung und auf Ebene der Proteinexpression mittels Immunblot-Analyse charakterisiert. Sowohl auf Ebene der mRNA- als auch Protein-Expression zeigten CNIH-2/3 eine besonders starke Expression in der frühen Ontogenese, die mit zunehmendem Alter abnahm. Dagegen verhielten sich die porenbildenden AMPA-Rezeptor Untereinheiten GluA1-4 und auch ihre prototypischen Hilfsuntereinheiten, wie die *Transmembrane AMPA-receptor Regulatory Proteins* (TARPs) genau entgegengesetzt. Ihre Expression nahm im Entwicklungsverlauf zu. Depletierende Ko-Immunpräzipitationen der porenbildenden AMPA-Rezeptor-Untereinheiten GluA1-4 offenbarten, dass CNIH-2/3 im Verlauf der Entwicklung in gleich bleibender Stöchiometrie in AMPA-Rezeptorkomplexe integriert ist. Somit verbleibt in der frühen Ontogenese ein signifikanter Anteil an CNIH-2/3, der nicht mit AMPA-

Rezeptoren interagiert. Dieser AMPA-Rezeptor-freie Anteil an CNIH-2/3 steht für andere Funktionen als die einer AMPA-Rezeptor Hilfsuntereinheit zur Verfügung.
Zusammengefasst zeigt die folgende Arbeit, dass CNIH-2/3 sowohl als ER Frachtexporter fungieren als auch – bei Anwesenheit von AMPA-Rezeptoren - als deren Hilfsuntereinheit in Rezeptorkomplexe an der Zelloberfäche rekrutiert werden. Die reziproken Expressionsprofile der porenbildenden AMPA-Rezeptoren-Untereinheiten und CNIH-2/3 bei jedoch unveränderter anteiliger Zusammensetzung der Rezeptorkomplexe während der Ontogenese deuten auf eine zusätzliche Funktion von CNIH-2/3 – z. B. als ER Frachtexporter von Wachstumsfaktoren – während der frühen Entwicklung hin.

7. Literature

Altman, J. B. S. A. (1997). Development of the Cerebellar System. In Relation to Its Evolution, Structure, and Functions. CRC Press**:** 783.

Angevine, J. B., Jr. and R. L. Sidman (1961). "Autoradiographic study of cell migration during histogenesis of cerebral cortex in the mouse." Nature **192**: 766-768.

Anggono, V. and R. L. Huganir (2012). "Regulation of AMPA receptor trafficking and synaptic plasticity." Current Opinion in Neurobiology **22**(3): 461-469.

Anton, E. S., H. T. Ghashghaei, et al. (2004). "Receptor tyrosine kinase ErbB4 modulates neuroblast migration and placement in the adult forebrain." Nature Neuroscience **7**(12): 1319-1328.

Aridor, M., S. I. Bannykh, et al. (1995). "Sequential coupling between COPII and COPI vesicle coats in endoplasmic reticulum to Golgi transport." Journal of Cell Biology **131**(4): 875-893.

Ayalon, G. and Y. Stern-Bach (2001). "Functional assembly of AMPA and kainate receptors is mediated by several discrete protein-protein interactions." Neuron **31**(1): 103-113.

Baude, A., E. Molnar, et al. (1994). "Synaptic and nonsynaptic localization of the GluR1 subunit of the AMPA-type excitatory amino acid receptor in the rat cerebellum." Journal of Neuroscience **14**(5 Pt 1): 2830-2843.

Bentivoglio, M. and P. Mazzarello (1999). "The history of radial glia." Brain Res Bull **49**(5): 305-315.

Bhardwaj, N. and H. Lu (2005). "Correlation between gene expression profiles and protein-protein interactions within and across genomes." Bioinformatics **21**(11): 2730-2738.

Bliss, T. V. and A. R. Gardner-Medwin (1973). "Long-lasting potentiation of synaptic transmission in the dentate area of the unanaestetized rabbit following stimulation of the perforant path." J Physiol **232**(2): 357-374.

Bokel, C., S. Dass, et al. (2006). "Drosophila Cornichon acts as cargo receptor for ER export of the TGFalpha-like growth factor Gurken." Development **133**(3): 459-470.

Brockie, P. J. and A. V. Maricq (2010). "In a pickle: is cornichon just relish or part of the main dish?" Neuron **68**(6): 1017-1019.

Castro, C. P., D. Piscopo, et al. (2007). "Cornichon regulates transport and secretion of TGFalpha-related proteins in metazoan cells." J Cell Sci **120**(Pt 14): 2454-2466.

Chang, S. and P. De Camilli (2001). "Glutamate regulates actin-based motility in axonal filopodia." Nat Neurosci **4**(8): 787-793.

Chen, W., R. Prithviraj, et al. (2009). "AMPA glutamate receptor subunits 1 and 2 regulate dendrite complexity and spine motility in neurons of the developing neocortex." Neuroscience **159**(1): 172-182.

Chung, H. J., J. Xia, et al. (2000). "Phosphorylation of the AMPA receptor subunit GluR2 differentially regulates its interaction with PDZ domain-containing proteins." Journal of Neuroscience **20**(19): 7258-7267.

Coleman, S. K., C. Cai, et al. (2003). "Surface expression of GluR-D AMPA receptor is dependent on an interaction between its C-terminal domain and a 4.1 protein." Journal of Neuroscience **23**(3): 798-806.

Conti, F., A. Minelli, et al. (1994). "Cellular localization and laminar distribution of AMPA glutamate receptor subunits mRNAs and proteins in the rat cerebral cortex." J Comp Neurol **350**(2): 241-259.

Cottrell, J. R., G. R. Dube, et al. (2000). "Distribution, density, and clustering of functional glutamate receptors before and after synaptogenesis in hippocampal neurons." J Neurophysiol **84**(3): 1573-1587.

Deitmer, J. W. and C. R. Rose (2010). "Ion changes and signalling in perisynaptic glia." Brain Res Rev **63**(1-2): 113-129.

Dev, K. K., A. Nishimune, et al. (1999). "The protein kinase C alpha binding protein PICK1 interacts with short but not long form alternative splice variants of AMPA receptor subunits." Neuropharmacology **38**(5): 635-644.

Diaz, A. L. and J. G. Gleeson (2009). "The molecular and genetic mechanisms of neocortex development." Clin Perinatol **36**(3): 503-512.

Fischer, M., S. Kaech, et al. (2000). "Glutamate receptors regulate actin-based plasticity in dendritic spines." Nat Neurosci **3**(9): 887-894.

Frerking, M. and R. A. Nicoll (2000). "Synaptic kainate receptors." Current Opinion in Neurobiology **10**(3): 342-351.

Fuchs, E. C., A. R. Zivkovic, et al. (2007). "Recruitment of parvalbumin-positive interneurons determines hippocampal function and associated behavior." Neuron **53**(4): 591-604.

Fukaya, M., M. Yamazaki, et al. (2005). "Spatial diversity in gene expression for VDCCgamma subunit family in developing and adult mouse brains." Neurosci Res **53**(4): 376-383.

Gallo, V., L. M. Upson, et al. (1992). "Molecular cloning and development analysis of a new glutamate receptor subunit isoform in cerebellum." Journal of Neuroscience **12**(3): 1010-1023.

Gallo, V., J. M. Zhou, et al. (1996). "Oligodendrocyte progenitor cell proliferation and lineage progression are regulated by glutamate receptor-mediated K+ channel block." J Neurosci **16**(8): 2659-2670.

Gill, M. B., A. S. Kato, et al. (2011). "Cornichon-2 modulates AMPA receptor-transmembrane AMPA receptor regulatory protein assembly to dictate gating and pharmacology." J Neurosci **31**(18): 6928-6938.

Gill, M. B., A. S. Kato, et al. (2012). "AMPA receptor modulation by cornichon-2 dictated by transmembrane AMPA receptor regulatory protein isoform." Eur J Neurosci **35**(2): 182-194.

Goldowitz, D. and K. Hamre (1998). "The cells and molecules that make a cerebellum." Trends in Neurosciences **21**(9): 375-382.

Golshani, P., J. T. Goncalves, et al. (2009). "Internally mediated developmental desynchronization of neocortical network activity." Journal of Neuroscience **29**(35): 10890-10899.

Gotz, M. and W. B. Huttner (2005). "The cell biology of neurogenesis." Nat Rev Mol Cell Biol **6**(10): 777-788.

Granger, A. J., Y. Shi, et al. (2013). "LTP requires a reserve pool of glutamate receptors independent of subunit type." Nature **493**(7433): 495-500.

Greger, I. H., P. Akamine, et al. (2006). "Developmentally regulated, combinatorial RNA processing modulates AMPA receptor biogenesis." Neuron **51**(1): 85-97.

Greger, I. H., L. Khatri, et al. (2003). "AMPA receptor tetramerization is mediated by Q/R editing." Neuron **40**(4): 763-774.

Greger, I. H., L. Khatri, et al. (2002). "RNA editing at arg607 controls AMPA receptor exit from the endoplasmic reticulum." Neuron **34**(5): 759-772.

Groc, L., B. Gustafsson, et al. (2002). "Spontaneous unitary synaptic activity in CA1 pyramidal neurons during early postnatal development: constant contribution of AMPA and NMDA receptors." J Neurosci **22**(13): 5552-5562.

Groc, L., B. Gustafsson, et al. (2006). "AMPA signalling in nascent glutamatergic synapses: there and not there!" Trends Neurosci **29**(3): 132-139.

Gupta, A., L. H. Tsai, et al. (2002). "Life is a journey: a genetic look at neocortical development." Nat Rev Genet **3**(5): 342-355.

Hamad, M. I., Z. L. Ma-Hogemeier, et al. (2011). "Cell class-specific regulation of neocortical dendrite and spine growth by AMPA receptor splice and editing variants." Development **138**(19): 4301-4313.

Harmel, N., B. Cokic, et al. (2012). "AMPA receptors commandeer an ancient cargo exporter for use as an auxiliary subunit for signaling." PLoS One **7**(1): e30681.

Hatten, M. E. (1999). "Central nervous system neuronal migration." Annu Rev Neurosci **22**: 511-539.

Heine, M., O. Thoumine, et al. (2008). "Activity-independent and subunit-specific recruitment of functional AMPA receptors at neurexin/neuroligin contacts." Proc Natl Acad Sci U S A **105**(52): 20947-20952.

Herring, B. E., Y. Shi, et al. (2013). "Cornichon proteins determine the subunit composition of synaptic AMPA receptors." Neuron **77**(6): 1083-1096.

Higuchi, M., S. Maas, et al. (2000). "Point mutation in an AMPA receptor gene rescues lethality in mice deficient in the RNA-editing enzyme ADAR2." Nature **406**(6791): 78-81.

Hollmann, M. and S. Heinemann (1994). "Cloned glutamate receptors." Annu Rev Neurosci **17**: 31-108.

Hollmann, M., C. Maron, et al. (1994). "N-glycosylation site tagging suggests a three transmembrane domain topology for the glutamate receptor GluR1." Neuron **13**(6): 1331-1343.

Hoshino, H., T. Uchida, et al. (2007). "Cornichon-like protein facilitates secretion of HB-EGF and regulates proper development of cranial nerves." Mol Biol Cell **18**(4): 1143-1152.

Hunter, C., R. S. Petralia, et al. (1993). "Expression of AMPA-selective glutamate receptor subunits in morphologically defined neurons of the mammalian cochlear nucleus." Journal of Neuroscience **13**(5): 1932-1946.

Isaac, J. T., M. C. Ashby, et al. (2007). "The role of the GluR2 subunit in AMPA receptor function and synaptic plasticity." Neuron **54**(6): 859-871.

Jackson, A. C. and R. A. Nicoll (2011). "The expanding social network of ionotropic glutamate receptors: TARPs and other transmembrane auxiliary subunits." Neuron **70**(2): 178-199.

Jakowec, M. W., L. Yen, et al. (1995). "In situ hybridization analysis of AMPA receptor subunit gene expression in the developing rat spinal cord." Neuroscience **67**(4): 909-920.

Jansson, L. C., H. K. Wigren, et al. (2011). "Functional alpha-amino-3-hydroxy-5-methylisoxazole-4-propionic acid receptors in differentiating embryonic neural progenitor cells." Neuroreport **22**(6): 282-287.

Jonas, P., C. Racca, et al. (1994). "Differences in Ca2+ permeability of AMPA-type glutamate receptor channels in neocortical neurons caused by differential GluR-B subunit expression." Neuron **12**(6): 1281-1289.

Kato, A. S., M. B. Gill, et al. (2010). "Hippocampal AMPA receptor gating controlled by both TARP and cornichon proteins." Neuron **68**(6): 1082-1096.

Kato, A. S., M. B. Gill, et al. (2010). "TARPs differentially decorate AMPA receptors to specify neuropharmacology." Trends Neurosci **33**(5): 241-248.

Kerchner, G. A. and R. A. Nicoll (2008). "Silent synapses and the emergence of a postsynaptic mechanism for LTP." Nat Rev Neurosci **9**(11): 813-825.

Koike, M., S. Tsukada, et al. (2000). "Regulation of kinetic properties of GluR2 AMPA receptor channels by alternative splicing." Journal of Neuroscience **20**(6): 2166-2174.

Kornblum, H. I., S. D. Zurcher, et al. (1999). "Multiple trophic actions of heparin-binding epidermal growth factor (HB-EGF) in the central nervous system." European Journal of Neuroscience **11**(9): 3236-3246.

Kriegstein, A. R. and S. C. Noctor (2004). "Patterns of neuronal migration in the embryonic cortex." Trends in Neurosciences **27**(7): 392-399.

Kumar, S. S., A. Bacci, et al. (2002). "A developmental switch of AMPA receptor subunits in neocortical pyramidal neurons." J Neurosci **22**(8): 3005-3015.

Lee, M. C. and E. A. Miller (2007). "Molecular mechanisms of COPII vesicle formation." Semin Cell Dev Biol **18**(4): 424-434.

Leuschner, W. D. and W. Hoch (1999). "Subtype-specific assembly of alpha-amino-3-hydroxy-5-methyl-4-isoxazole propionic acid receptor subunits is mediated by their n-terminal domains." Journal of Biological Chemistry **274**(24): 16907-16916.

Lidow, M. S. and F. Wang (1995). "Neurotransmitter receptors in the developing cerebral cortex." Crit Rev Neurobiol **9**(4): 395-418.

Lomeli, H., J. Mosbacher, et al. (1994). "Control of kinetic properties of AMPA receptor channels by nuclear RNA editing." Science **266**(5191): 1709-1713.

Lomeli, H., R. Sprengel, et al. (1993). "The rat delta-1 and delta-2 subunits extend the excitatory amino acid receptor family." FEBS Lett **315**(3): 318-322.

LoTurco, J. J., D. F. Owens, et al. (1995). "GABA and glutamate depolarize cortical progenitor cells and inhibit DNA synthesis." Neuron **15**(6): 1287-1298.

Malinow, R. and R. C. Malenka (2002). "AMPA receptor trafficking and synaptic plasticity." Annu Rev Neurosci **25**: 103-126.

Manent, J. B., I. Jorquera, et al. (2006). "Glutamate acting on AMPA but not NMDA receptors modulates the migration of hippocampal interneurons." J Neurosci **26**(22): 5901-5909.

Maric, D., Q. Y. Liu, et al. (2000). "Functional ionotropic glutamate receptors emerge during terminal cell division and early neuronal differentiation of rat neuroepithelial cells." J Neurosci Res **61**(6): 652-662.

Martin, L. J., A. Furuta, et al. (1998). "AMPA receptor protein in developing rat brain: glutamate receptor-1 expression and localization change at regional, cellular, and subcellular levels with maturation." Neuroscience **83**(3): 917-928.

Martins, R. A., R. Linden, et al. (2006). "Glutamate regulates retinal progenitors cells proliferation during development." Eur J Neurosci **24**(4): 969-980.

Matsuda, S., E. Miura, et al. (2008). "Accumulation of AMPA receptors in autophagosomes in neuronal axons lacking adaptor protein AP-4." Neuron **57**(5): 730-745.

Mauric, V., A. Molders, et al. (2013). "Ontogeny repeats the phylogenetic recruitment of the cargo exporter cornichon into AMPA receptor signaling complexes." Mol Cell Neurosci **56C**: 10-17.

McKinney, R. A., M. Capogna, et al. (1999). "Miniature synaptic events maintain dendritic spines via AMPA receptor activation." Nat Neurosci **2**(1): 44-49.

Menuz, K., G. A. Kerchner, et al. (2009). "Critical role for TARPs in early development despite broad functional redundancy." Neuropharmacology **56**(1): 22-29.

Metin, C., J. P. Denizot, et al. (2000). "Intermediate zone cells express calcium-permeable AMPA receptors and establish close contact with growing axons." J Neurosci **20**(2): 696-708.

Miale, I. L. and R. L. Sidman (1961). "An autoradiographic analysis of histogenesis in the mouse cerebellum." Exp Neurol **4**: 277-296.

Monyer, H., P. H. Seeburg, et al. (1991). "Glutamate-operated channels: developmentally early and mature forms arise by alternative splicing." Neuron **6**(5): 799-810.

Moss, S. J., C. D. Blackstone, et al. (1993). "Phosphorylation of recombinant non-NMDA glutamate receptors on serine and tyrosine residues." Neurochemical Research **18**(1): 105-110.

Naeve, G. S., M. Ramakrishnan, et al. (1997). "Neuritin: a gene induced by neural activity and neurotrophins that promotes neuritogenesis." Proc Natl Acad Sci U S A **94**(6): 2648-2653.

Nguyen, L., J. M. Rigo, et al. (2001). "Neurotransmitters as early signals for central nervous system development." Cell Tissue Res **305**(2): 187-202.

Ni, X., G. J. Sullivan, et al. (2007). "Developmental characteristics of AMPA receptors in chick lumbar motoneurons." Developmental Neurobiology **67**(11): 1419-1432.

Ouardouz, M., E. Coderre, et al. (2009). "Glutamate receptors on myelinated spinal cord axons: II. AMPA and GluR5 receptors." Ann Neurol **65**(2): 160-166.

Passafaro, M., T. Nakagawa, et al. (2003). "Induction of dendritic spines by an extracellular domain of AMPA receptor subunit GluR2." Nature **424**(6949): 677-681.

Pellegrini-Giampietro, D. E., M. V. Bennett, et al. (1991). "Differential expression of three glutamate receptor genes in developing rat brain: an in situ hybridization study." Proc Natl Acad Sci U S A **88**(10): 4157-4161.

Penn, A. C., S. R. Williams, et al. (2008). "Gating motions underlie AMPA receptor secretion from the endoplasmic reticulum." Embo Journal **27**(22): 3056-3068.

Petralia, R. S., J. A. Esteban, et al. (1999). "Selective acquisition of AMPA receptors over postnatal development suggests a molecular basis for silent synapses." Nat Neurosci **2**(1): 31-36.

Pinto-Lord, M. C., P. Evrard, et al. (1982). "Obstructed neuronal migration along radial glial fibers in the neocortex of the reeler mouse: a Golgi-EM analysis." Brain Research **256**(4): 379-393.

Platel, J. C., B. Lacar, et al. (2007). "GABA and glutamate signaling: homeostatic control of adult forebrain neurogenesis." J Mol Histol **38**(4): 303-311.

Platel, J. C., B. Lacar, et al. (2007). "GABA and glutamate signaling: homeostatic control of adult forebrain neurogenesis." J Mol Histol **38**(6): 602-610.

Powers, J. and C. Barlowe (1998). "Transport of axl2p depends on erv14p, an ER-vesicle protein related to the Drosophila cornichon gene product." J Cell Biol **142**(5): 1209-1222.

Putz, U., C. Harwell, et al. (2005). "Soluble CPG15 expressed during early development rescues cortical progenitors from apoptosis." Nature Neuroscience **8**(3): 322-331.

Qiu, S., L. F. Zhao, et al. (2006). "Differential reelin-induced enhancement of NMDA and AMPA receptor activity in the adult hippocampus." Journal of Neuroscience **26**(50): 12943-12955.

Rao, M. S. J., M. (2005). "Developmental Neurobiology." Springer: 424.

Resende, R. R., A. Adhikari, et al. (2010). "Influence of spontaneous calcium events on cell-cycle progression in embryonal carcinoma and adult stem cells." Biochim Biophys Acta **1803**(2): 246-260.

Ripellino, J. A., R. L. Neve, et al. (1998). "Expression and heteromeric interactions of non-N-methyl-D-aspartate glutamate receptor subunits in the developing and adult cerebellum." Neuroscience **82**(2): 485-497.

Ripley, B., S. Otto, et al. (2011). "Regulation of synaptic stability by AMPA receptor reverse signaling." Proc Natl Acad Sci U S A **108**(1): 367-372.

Risher, W. C. and C. Eroglu (2012). "Thrombospondins as key regulators of synaptogenesis in the central nervous system." Matrix Biol **31**(3): 170-177.

Ritter, L. M., D. M. Vazquez, et al. (2002). "Ontogeny of ionotropic glutamate receptor subunit expression in the rat hippocampus." Brain Res Dev Brain Res **139**(2): 227-236.

Rodriguez, M., M. Sabate, et al. (2013). "The role of non-synaptic extracellular glutamate." Brain Res Bull **93**: 17-26.

Rohrbough, J. and N. C. Spitzer (1999). "Ca(2+)-permeable AMPA receptors and spontaneous presynaptic transmitter release at developing excitatory spinal synapses." J Neurosci **19**(19): 8528-8541.

Root, C. M., N. A. Velazquez-Ulloa, et al. (2008). "Embryonically expressed GABA and glutamate drive electrical activity regulating neurotransmitter specification." Journal of Neuroscience **28**(18): 4777-4784.

Rosenmund, C., Y. Stern-Bach, et al. (1998). "The tetrameric structure of a glutamate receptor channel." Science **280**(5369): 1596-1599.

Roth, S., F. S. Neuman-Silberberg, et al. (1995). "cornichon and the EGF receptor signaling process are necessary for both anterior-posterior and dorsal-ventral pattern formation in Drosophila." Cell **81**(6): 967-978.

Saab, A. S., A. Neumeyer, et al. (2012). "Bergmann glial AMPA receptors are required for fine motor coordination." Science **337**(6095): 749-753.

Sasaki, T., N. Matsuki, et al. (2011). "Action-potential modulation during axonal conduction." Science **331**(6017): 599-601.

Sato, K., H. Kiyama, et al. (1993). "The differential expression patterns of messenger RNAs encoding non-N-methyl-D-aspartate glutamate receptor subunits (GluR1-4) in the rat brain." Neuroscience **52**(3): 515-539.

Schwenk, J., N. Harmel, et al. (2012). "High-resolution proteomics unravel architecture and molecular diversity of native AMPA receptor complexes." Neuron **74**(4): 621-633.

Schwenk, J., N. Harmel, et al. (2009). "Functional proteomics identify cornichon proteins as auxiliary subunits of AMPA receptors." Science **323**(5919): 1313-1319.

Shi, Y., Y. H. Suh, et al. (2010). "Functional comparison of the effects of TARPs and cornichons on AMPA receptor trafficking and gating." Proc Natl Acad Sci U S A **107**(37): 16315-16319.

Smith, T. C., L. Y. Wang, et al. (2000). "Heterogeneous conductance levels of native AMPA receptors." Journal of Neuroscience **20**(6): 2073-2085.

Sommer, B., K. Keinanen, et al. (1990). "Flip and flop: a cell-specific functional switch in glutamate-operated channels of the CNS." Science **249**(4976): 1580-1585.

Song, I. and R. L. Huganir (2002). "Regulation of AMPA receptors during synaptic plasticity." Trends in Neurosciences **25**(11): 578-588.

Stern-Bach, Y., B. Bettler, et al. (1994). "Agonist selectivity of glutamate receptors is specified by two domains structurally related to bacterial amino acid-binding proteins." Neuron **13**(6): 1345-1357.

Storrie, B., J. White, et al. (1998). "Recycling of golgi-resident glycosyltransferases through the ER reveals a novel pathway and provides an explanation for nocodazole-induced Golgi scattering." Journal of Cell Biology **143**(6): 1505-1521.

Stys, P. K. (2011). "The axo-myelinic synapse." Trends Neurosci **34**(8): 393-400.

Super, H. and H. B. Uylings (2001). "The early differentiation of the neocortex: a hypothesis on neocortical evolution." Cereb Cortex **11**(12): 1101-1109.

Suzuki, E., M. Kessler, et al. (2008). "The fast kinetics of AMPA GluR3 receptors is selectively modulated by the TARPs gamma 4 and gamma 8." Mol Cell Neurosci **38**(1): 117-123.

Szul, T. and E. Sztul (2011). "COPII and COPI traffic at the ER-Golgi interface." Physiology (Bethesda) **26**(5): 348-364.

Takago, H., Y. Nakamura, et al. (2005). "G protein-dependent presynaptic inhibition mediated by AMPA receptors at the calyx of Held." Proc Natl Acad Sci U S A **102**(20): 7368-7373.

Terhag, J., K. Gottschling, et al. (2010). "The Transmembrane Domain C of AMPA Receptors is Critically Involved in Receptor Function and Modulation." Front Mol Neurosci **3**: 117.

Tichelaar, W., M. Safferling, et al. (2004). "The Three-dimensional Structure of an Ionotropic Glutamate Receptor Reveals a Dimer-of-dimers Assembly." Journal of Molecular Biology **344**(2): 435-442.

Tissir, F. and A. M. Goffinet (2003). "Reelin and brain development." Nature Reviews Neuroscience **4**(6): 496-505.

Toki, F., D. Nanba, et al. (2005). "Ectodomain shedding of membrane-anchored heparin-binding EGF like growth factor and subcellular localization of the C-terminal fragment in the cell cycle." J Cell Physiol **202**(3): 839-848.

Tomita, S. (2010). "Regulation of ionotropic glutamate receptors by their auxiliary subunits." Physiology (Bethesda) **25**(1): 41-49.

Tomita, S., L. Chen, et al. (2003). "Functional studies and distribution define a family of transmembrane AMPA receptor regulatory proteins." J Cell Biol **161**(4): 805-816.

Tracy, T. E., J. J. Yan, et al. (2011). "Acute knockdown of AMPA receptors reveals a trans-synaptic signal for presynaptic maturation." EMBO J **30**(8): 1577-1592.

Traynelis, S. F., L. P. Wollmuth, et al. (2010). "Glutamate receptor ion channels: structure, regulation, and function." Pharmacol Rev **62**(3): 405-496.

Tsuzuki, K., B. Lambolez, et al. (2001). "Absolute quantification of AMPA receptor subunit mRNAs in single hippocampal neurons." Journal of Neurochemistry **77**(6): 1650-1659.

van den Pol, A. N., K. Obrietan, et al. (1995). "Embryonic hypothalamic expression of functional glutamate receptors." Neuroscience **67**(2): 419-439.

Van Dolah, F. M. and J. S. Ramsdell (1996). "Maitotoxin, a calcium channel activator, inhibits cell cycle progression through the G1/S and G2/M transitions and prevents CDC2 kinase activation in GH4C1 cells." J Cell Physiol **166**(1): 49-56.

von Engelhardt, J., V. Mack, et al. (2010). "CKAMP44: a brain-specific protein attenuating short-term synaptic plasticity in the dentate gyrus." Science **327**(5972): 1518-1522.

Wang, F., R. Liu, et al. (2007). "Heparin-binding EGF-like growth factor is an early response gene to chemotherapy and contributes to chemotherapy resistance." Oncogene **26**(14): 2006-2016.

Wang, F., C. Sloss, et al. (2007). "Membrane-bound heparin-binding epidermal growth factor like growth factor regulates E-cadherin expression in pancreatic carcinoma cells." Cancer Research **67**(18): 8486-8493.

Ward, T. H., R. S. Polishchuk, et al. (2001). "Maintenance of Golgi structure and function depends on the integrity of ER export." Journal of Cell Biology **155**(4): 557-570.

Wenthold, R. J., R. S. Petralia, et al. (1996). "Evidence for multiple AMPA receptor complexes in hippocampal CA1/CA2 neurons." Journal of Neuroscience **16**(6): 1982-1989.

Whitney, N. P., H. Peng, et al. (2008). "Calcium-permeable AMPA receptors containing Q/R-unedited GluR2 direct human neural progenitor cell differentiation to neurons." FASEB J **22**(8): 2888-2900.

Wu, G., R. Malinow, et al. (1996). "Maturation of a central glutamatergic synapse." Science **274**(5289): 972-976.

Yan, D. and S. Tomita (2012). "Defined criteria for auxiliary subunits of glutamate receptors." J Physiol **590**(Pt 1): 21-31.

8. Acknowledgements

I would like to express my sincerest gratitude to my supervisor Prof. Dr. med. Nikolaj Klöcker for giving me the opportunity to carry out my research interests under his guidance, and for being a constructive critic in the best sense.

I would also like to thank Prof. Dr. rer. nat. C. R. Rose for attending the dissertation as second supervisor.

Also I would like to give my thanks to Dr. Henrike Berkefeld and Dr. Gerd Zolles for conducting the electrophysiological experiments, Dr. Nadine Harmel for good cooperation and Andrea Mölders for providing the real-time data. I am further grateful to Prof. Dr. rer. nat. Bernd Heimrich for the perfusion of rats and valuable hints and discussion.

Thanks to my colleagues Dr. Annett Schröter, Dr. Olaf Kletke, Dr. Fatih Demir, Dr. Shuping Wen, Dr. Angela Orth for proof reading and support. Special thanks to Simon Klapper for discussion and to Claudia Wittrock for help and support.